**GEOLOGICAL SURVEY OF CANADA
OPEN FILE 8640**

Summary of 2018 Mackenzie Delta Permafrost Field Campaign (mCAN2018), Northwest Territories

**Edited by
J. Boike and S.R. Dallimore**

2019

Canada

GEOLOGICAL SURVEY OF CANADA
OPEN FILE 8640

Summary of 2018 Mackenzie Delta Permafrost Field Campaign (mCAN2018), Northwest Territories

Edited by
J. Boike[1] and S.R. Dallimore[2]

[1]Alfred-Wegener-Institut, Helmholtz-Zentrum für Polar- und Meeresforschung, Postfach 120161, 27515 Bremerhaven, GERMANY
[2]Geological Survey of Canada, 9860 West Saanich Road, Sidney, British Columbia V8L 4B2

2019

TABLE OF CONTENTS

Summary of 2018 Mackenzie Delta Permafrost Field Campaign (mCAN2018)

CHAPTER 1 - Introduction

Boike, J. and Dallimore, S.R.

The Arctic is experiencing the effects of climate change with increasing air temperatures, fluctuations in seasonal sea ice cover and changing precipitation trends. As shown on Figure 1, surface air temperatures in the western Arctic of North America and northern Siberia have warmed by up to 4°C in the past 5 decades, a rate that is more than twice the global average. Consequent changes are also occurring in the permafrost interval with observations compiled by the Global Terrestrial Network for Permafrost indicating significant warming of permafrost in the past decade (Biskaborn et al., 2019).
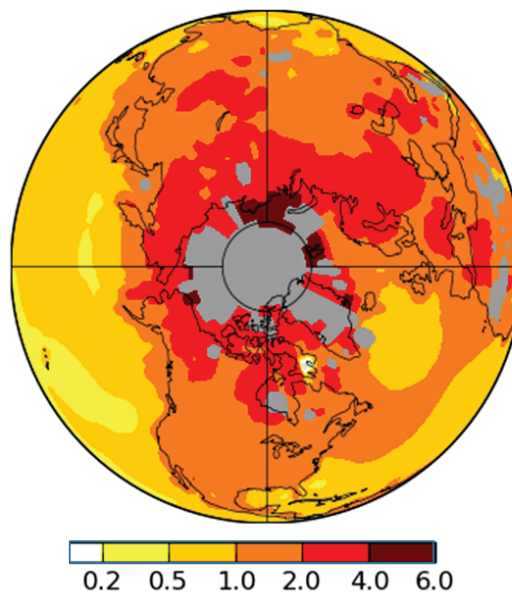
Figure 1: Polar projection of trends in annual temperature data from 1968 to 2018 generated from Goddard Institute for Space Studies GISS Surface Temperature Analysis v4 database (https://data.giss.nasa.gov/gistemp/) using 250 km smoothing radius.

In the western Arctic of Canada, along the Beaufort Sea coast, there is considerable interest in studying permafrost response to ongoing climate change as this area is underlain by ice-rich permafrost and it is presently experiencing rapid rates of coastal erosion and potential landscape response. Canadian and international research groups are attempting to quantify the response of permafrost to climate change and, in doing so, to provide information to northern residents and communities who are appraising associated geohazards and developing adaptation strategies. Similarly, there is interest in regional processes that may have global scale interconnections. Of particular interest, the carbon cycle of permafrost regions has been shown to be very sensitive to even short warming spells, snow cover duration and the amount of rainfall. Organic matter stored in previously frozen sediments can start to decompose, potentially releasing greenhouse gases into the atmosphere. These effects may potentially transform permafrost areas from a net sink to a net source of atmospheric carbon in the future (AMAP, 2015).

This Open File Report summarizes permafrost field activities undertaken jointly by Canadian and German researchers from August 13 to September 09, 2018. The field work was conducted in the Mackenzie Delta area along the Inuvik-Tuktoyaktuk Highway corridor and near the community of Tuktoyaktuk (Fig. 2). While the results we present are preliminary in nature, it is our goal to detail the research we have undertaken together and to provide guidance on our plans to release our field data sets. Central to this effort is our intent to report on our work to northerners.

Participant agencies and program description

The field work described in this report was realized as a collaboration between researchers from the Canadian government, Canadian academic groups and German research institutes. The Geological Survey of Canada's research program focussed on geohazard aspects related to coastal processes and goals to document nearshore bathymetry and quantify permafrost degradation. The Canadian Hydrographic Service contributed equipment and assisted with processing and interpretation of multibeam echo sounder surveys. The Aurora Research Institute provided logistics support and, with Royal Roads University, participated in the marine field work. Wilfred Laurier University and University of Guelph provided guidance on the selection of research sites as well as access to the Trail Valley Creek research facilities.

The participants from Germany were enabled through a technology program that constituted a module within the Modular Observation Solutions for Earth Systems (MOSES, https://www.ufz.de/moses/index.php?en=44537) project of the Helmholtz Association. This novel, modular and mobile observing system of the Helmholtz Association is jointly developed within the research field "Earth and Environment" and comprises highly flexible and mobile observation modules which are specifically designed to investigate the interactions of short-term events and long-term trends across Earth compartments. As a first test campaign, scientists, technicians and students of the MOSES event group "Thawing Permafrost", worked together in Northwest Territories (Fig. 2).

Contributing Authors

Author contact information by organization:

Authors	Affiliation and Address
Boike, J., Bussmann, I., Cable, W., Grünberg, I., Hartig, B., Hartmann, J., Helm, V., Lange, S., Overduin, P.P.	Alfred-Wegener-Institute Helmholtz Centre for Polar and Marine Research – AWI, Am Handelshafen 12 27570 Bremerhaven, GERMANY
Dallimore, S.R.[a] Couture, N. [b]	[a]Geological Survey of Canada-Pacific, Natural Resources Canada, 9860 West Saanich Rd., Sidney, BC, V8L 4B2, CANADA [b]Geological Survey of Canada-North, Natural Resources Canada, 601 Booth St., Ottawa, ON, KIA OE8, CANADA
Achterberg, P.E., Greinert, J., Kampmeier, M., Nehir, M., Weiss, T.	Helmholtz Centre for Ocean Research Kiel – GEOMAR, Wischhofstr. 1-3, 24148 Kiel, GERMANY
Haberland, C., Ryberg, T.	Helmholtz Centre Potsdam German Research Centre for Geosciences- GFZ, Telegrafenberg, 14473 Potsdam, GERMANY
Molloy, B., Dallimore, A.	Royal Roads University, 2005 Sooke Rd., Victoria, BC V9B 5Y2 CANADA
Youngblut, S.	Canadian Hydrographic Service, Fisheries and Oceans Canada, 867 Lakeshore Rd., Burlington, ON, L7S 1A1, CANADA
Amos, E.	Aurora Research Institute, 191 Mackenzie Road PO Box 1450, Inuvik, NT, X0E 0T0, CANADA
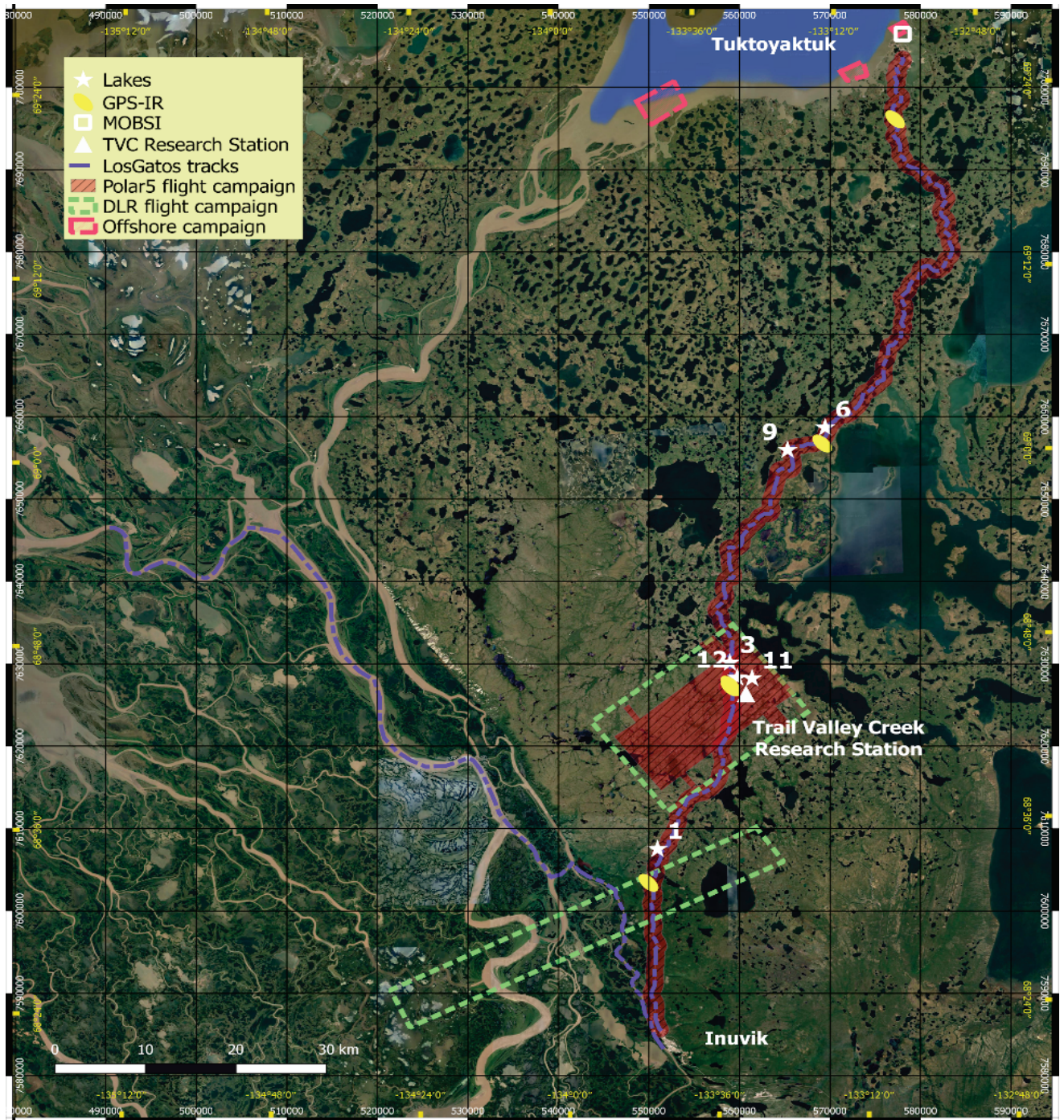
Figure 2: Overview map showing the study sites reached by car, foot and small boat during the MOSES "mCAN2018" campaign in August and September 2018. The areas covered by flight campaigns during August by AWI (Polar 5; LIDAR scanning, high resolution RGB images) and DLR (Tandem L) are shown as red and green dashed rectangles. The numbers indicate the investigated lakes (Lake 1, 3, 6, 9, 11 and 12). MOBSI: Mobile Ocean Bottom Seismometer, GPS-IR: GPS-IR: Interferometric Reflectometry, Los Gatos portable Greenhouse Gas Analyzer.

References:

Biskaborn, B.K., Smith, S.L., Noetzli, J., Matthes, H., Vieira, G., Streletskiy, D.A., Schoeneich, P., Romanovsky, V.E., and Lewkowicz, A.G. 2019. Permafrost is warming at a global scale. Nature Communications. doi:10.1038/s41467-018-08240-4.

AMAP. 2015. AMAP Assessment 2015: Methane as an Arctic climate forcer. AMAP, Oslo.

Acknowledgements:

CHAPTER 2 – Acoustic mapping of coastal areas near Tuktoyaktuk

Molloy, B., Dallimore, S.R., Youngblut, S., Kampmeier, M., Dallimore, A. and Amos, E.

Objectives

The Tuktoyaktuk area and its seaward coast are experiencing high rates of coastal erosion that potentially pose a hazard to infrastructure in the community and to marine operational activities. The scientific objective of our field work was to quantify the marine geomorphology and bathymetric changes in the nearshore environment and contribute to the understanding of the dominant geologic processes ongoing in this setting, such as thermokarst degradation in the nearshore, sediment transport, and ice scour.

Methodology and Fieldwork Summary

Multibeam echo sounder (MBES) surveys were conducted in August 2017 and 2018. A 5.2 m GSC survey launch was used in 2017 and a 6.7 m Aurora Research Institute launch was used in 2018. A pole-mounted Norbit iWBMSc multibeam system with operating frequency between 160-400 kHz was used for both field campaigns. The system is owned by the Canadian Hydrographic Service (CHS) with operations being conducted by the Geological Survey of Canada and Royal Roads University. All Norbit data were collected using the QPS QINCy acquistion software, which creates a file directory upon project setup so that incoming bathymetry data propagates the file folders automatically. While surveying, an AML sound velocity probe was used to collect the speed of sound through the water column. After each cast, the profiles collected were then uploaded to the field laptop using SeaCast software, then reformatted to .svp files for Caris and .csv files for QINCy, and finally saved in the SVP folder within the main project directory. Metadata files were collected daily using a CHS excel file format to recorde survey specific observations and saved in a metadata file within the main project directory. NRCan's Canadian Geodetic Survey Global Positioning System (GPS) base station data for Tuktoyaktuk were collected to enable corrections to position and motion data. Post-processing and cleaning of the multibeam data were undertaken by the CHS.

Preliminary results

The Tuktoyaktuk surveys focused on the approach to Tuktoyaktuk Harbour and the navigation channel of the main harbour itself, the area offshore of Tuktoyaktuk Island, the seaward extent of engineered shore line, and areas offshore of a large retrogressive thaw flow slide near Peninsula Point (Fig. 3). In general, the bathymetry of the research area was shallow (<10 m) with the exception of channels and localized dredged areas within the inner harbour that were up to 30 m deep. The Canadian Coast Guard (CCG) dock was utilized for docking the survey launches and

harbour surveys started and commenced each day from this site allowing en route surveying of the main navigation channel. The following sections introduce the main research areas, highlighting salient features.
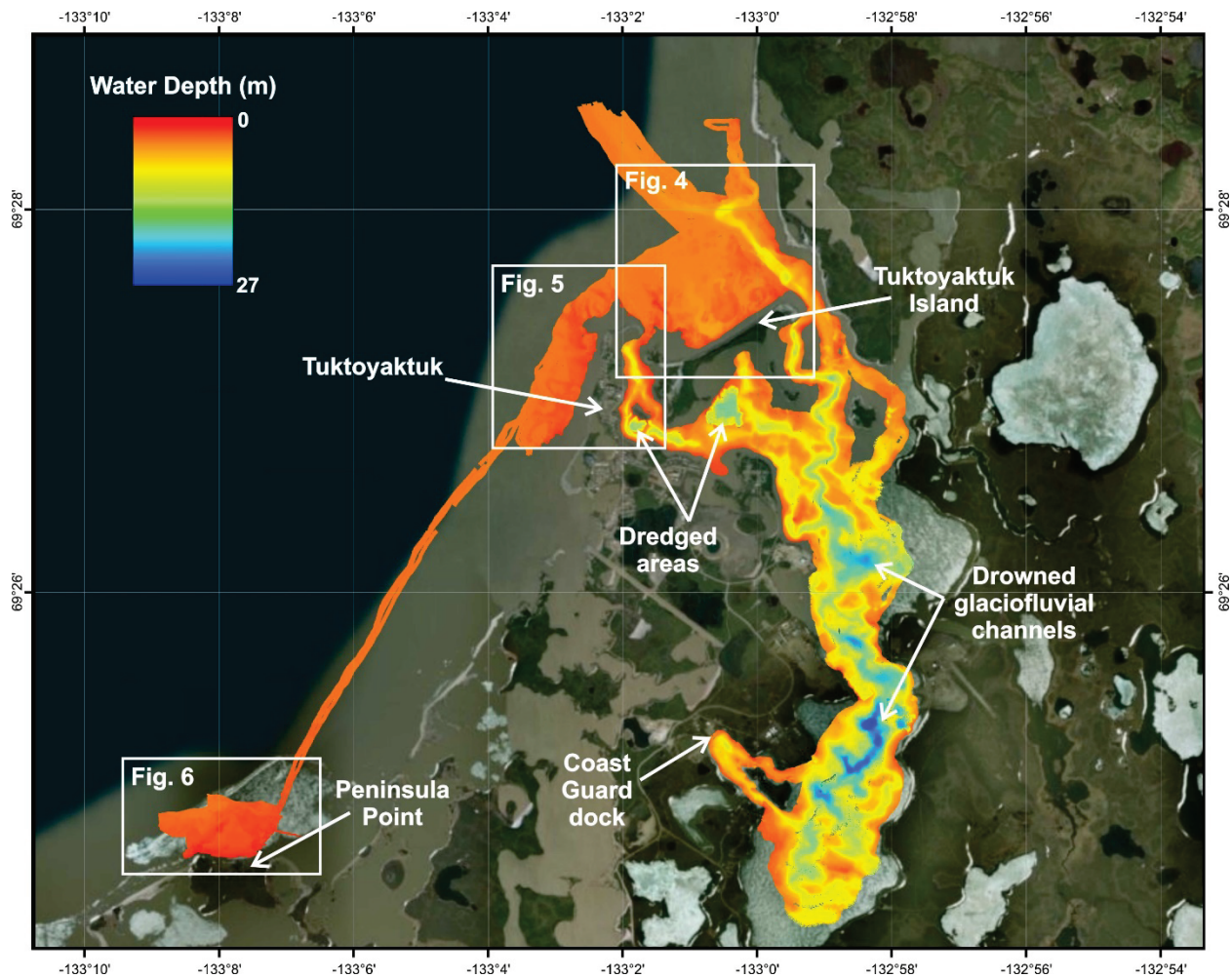
Figure 3: Location map showing multibeam bathymetry data collected during 2017 and 2018 field campaigns.

Tuktoyaktuk Harbour approaches

Sailing directions for Tuktoyaktuk Harbour identify an eastern and western entrance to the harbour, with the eastern entrance being the main navigation channel. The approach to the harbour from Kugmallit Bay is marked by navigation buoys with a controlling depth of ~4.4 m. Only small vessels are recommended to utilize the western harbour entrance. The strategy for the multibeam surveys was to map the western harbour entrance and the approach to the eastern channel that had been previously dredged. As shown on Figure 4, we observed that the west entrance to

7

4a)
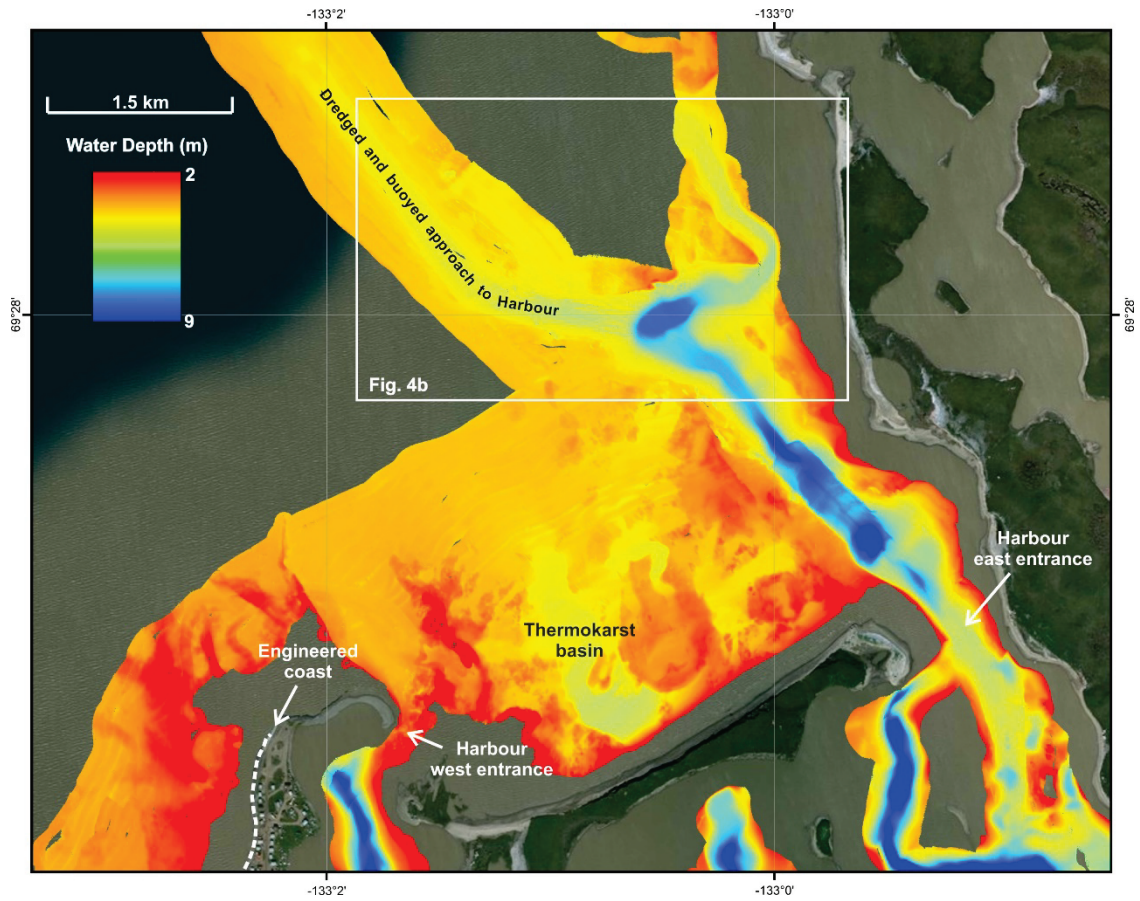
4b)
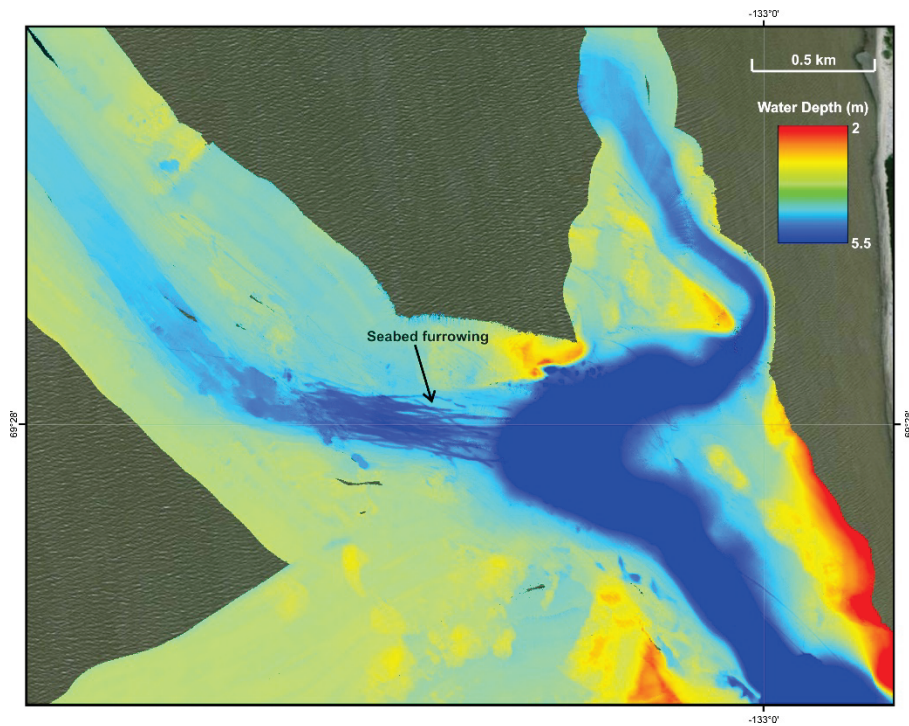
Figure 4: a) Bathymetry of approachs to Tuktoyaktuk Harbour and areas offshore of Tuktoyaktuk Island, b) enhancement of bathymetry of dredged channel area.

Tuktoyaktuk Harbour is very narrow and shallow, confirming that this entrance is only safe for small vessels in good weather conditions (Fig. 4). Our mapping of the buoyed approach to the east entrance to the harbour confirmed the shallow depth of this area with a narrow (~150 m) dredged channel connecting to a deep sinuous channel that continues to the main harbour area further to the south. The fidelity of the Norbit field data set allowed discrimination of subtle linear scour features that could be remnant features from past dredging, propeller marks or formed from possible ice scour (Fig. 4b).

Surveys offshore of Tuktoyaktuk Island

Tuktoyaktuk Island acts as a natural barrier protecting the harbour and community from the wave action and associated erosion. Recent investigations by Whalen (pers. com.) suggest that the island is eroding at an average rate of ~2 m/yr (2000-2015) and that at this rate, the island could be breached by 2035. The sediments comprising Tuktoyaktuk Island consist mainly of frozen sands with low ice contents. However, intervals of ice-rich strata have on occasion been exposed in the lower sections of the island close to sea level. In some areas of the island there is a thin, discontinuous cover of ice-rich diamicton. Several small retrogressive thaw flow slides have formed in this setting in the western part of the island.

The offshore bathymetry of Tuktoyaktuk Island reveals several well defined basins and pitted areas (Fig. 4a). In the shallow water areas immediately adjacent to the island there are also several sediment tongues extending into the nearshore from the eroding bluff. We envisage that this nearshore setting is undergoing thaw consolidation as the terrestrial permafrost has been transgressed and the mean annual bottom temperatures are above 0°C. As a consequence of these processes the main basin in front of Tuktoyaktuk Island may be a thermokarst basin. In contrast it is apparent that in the very nearshore, active sediment deposition is occurring both from the sandy sediments derived from cliff erosion and possible debris from retrogressive thaw flow slides.

Tuktoyaktuk Harbour surveys

The protected waters of Tuktoyaktuk Harbour near the community and south of the community have an interesting and varied morphology. The most obvious feature is a sinuous channel that deepens and widens toward the southern extent of the survey area. The channel has a maximum depth of >20 m (Fig. 3). This feature is interpreted as a drowned glaciofluvial channel that was formed during waning stages of deglaciation when sea level was much lower in the area than today. The influence of human activity is also apparent in the harbour area. Immediately south of Tuktoyaktuk Island there are several areas where sea floor dredging has occurred (Fig. 3). One of these was the source of fill material for the Tuktoyaktuk water reservoir that was constructed in the early 1980s.

The harbour area is recognized as a unique and important fish habitat as it is thought to be a nursery for Arctic cisco, a spawning area for Pacific herring and a year round habitat for whitefish. Sound velocity casts during our field survey confirmed that the water structure in the harbour area is quite complex with indications that the deeper basins trap cold saline waters, in sharp contrast to the overlying fresh water at the surface.

Eroding shore face offshore of community

The community of Tuktoyaktuk is located in a low lying coastal setting and has experienced significant coastal erosion throughout its history. In the 1980s, a variety of coastal engineering mitigation efforts were undertaken in an attempt to stabilize the west side of the peninsula where the community is located (Johnson, 2003). Unfortunately, in recent years these shore works have begun to fail and the erosion rates have increased, threatening existing infrastructure.

Recognizing the risk to the community, the Hamlet of Tuktoyaktuk has been relocating buildings from the exposed areas of the peninsula. The Hamlet is urgently seeking a longer term engineering solutions to protect the remaining infrastructure as well valued cultural places, such as the community grave yard. The bathymetric surveys conducted on the west side of the peninsula (Fig. 5) were undertaken to provide some modern base line information for engineers evaluating mitigation strategies.

Access to the very nearshore was limited due to the shallow water depths within approximately 250 m of the shoreline. This foreshore area consists of sandy sediments with evidence of considerable longshore sediment transport to the north. A ~9 km by 1.5 km area immediately offshore of the peninsula was surveyed (Fig. 5). In this area water depths were shallow (<4 m) with some small basins and arcuate sediment ridges that may be consistent with remnant shore line positions. A shallow bench area immediately offshore of the tip of the peninsula was inaccessible due to shallow water depths.
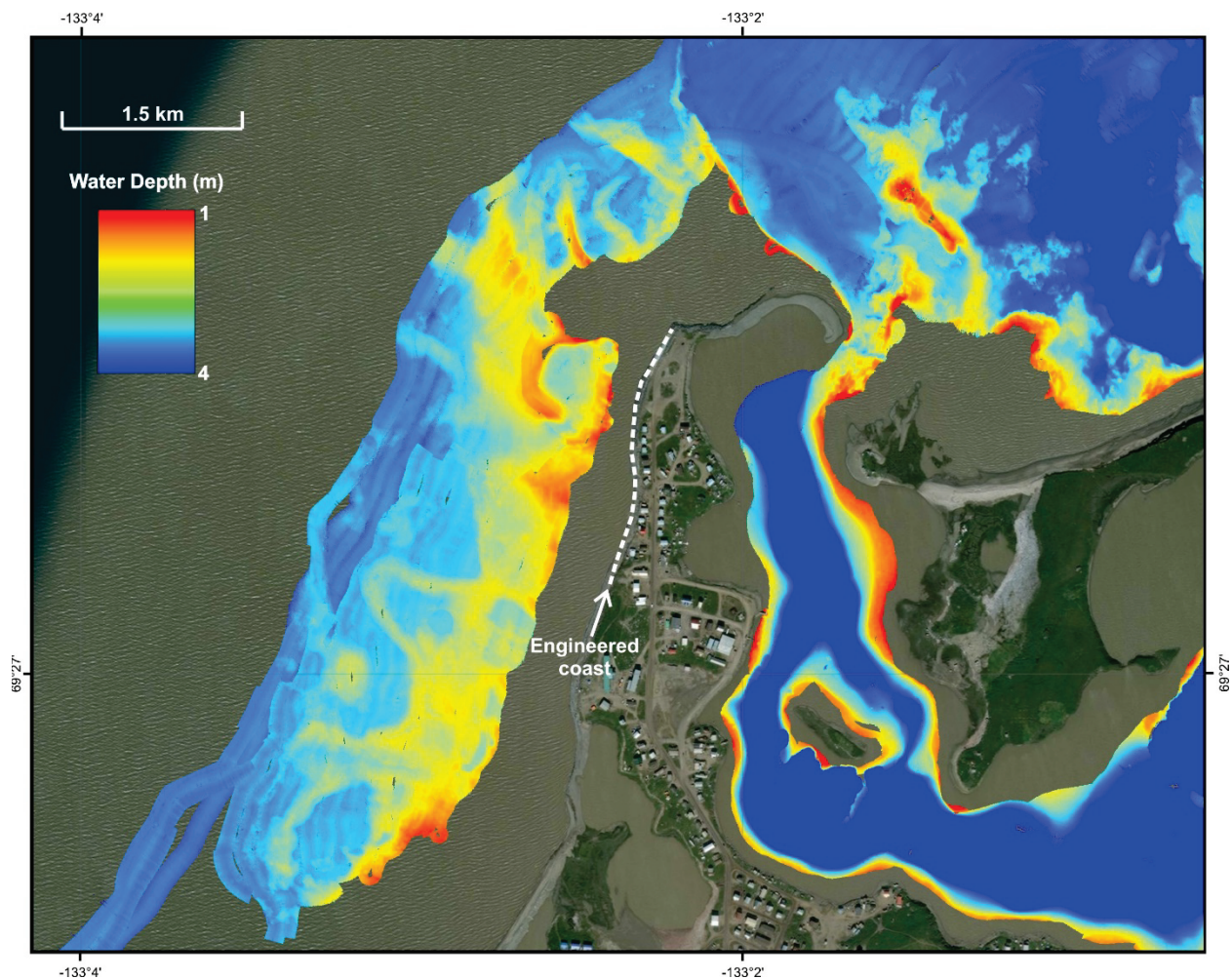
Figure 5: Bathymetry of area west of the Tuktoyaktuk community where coastal erosion in recent years has been particularly problematic.

Peninsula Point Surveys

Peninsula Point is a well-studied coastal permafrost site characterized by rapidly eroding ice-rich permafrost. As described by Mackay and Dallimore (1992) the cliff sediments are composed of a cover of 6-8 m of ice-rich glacial diamicton, overlying ~10 m of massive ice which in turn is underlain by coarse grained sands. Cliff erosion is primarily a consequence of retrogressive thaw flow slide activity with eroding ice-rich head walls and flows of liquefied sediment into the nearshore (Fig. 6). Our survey of the nearshore was undertaken to document if there was evidence of thermokarst activity in the nearshore area from thawing of ground ice below the seabed. As was observed offshore of Tuktoyaktuk Island there is a very well defined basin immediately offshore of the Island that has likely formed from permafrost thaw settlement in the

nearshore. A number of distinct terrestrial sediment flows emanating from the retrogressive thaw slide activity could also be traced into the nearshore.
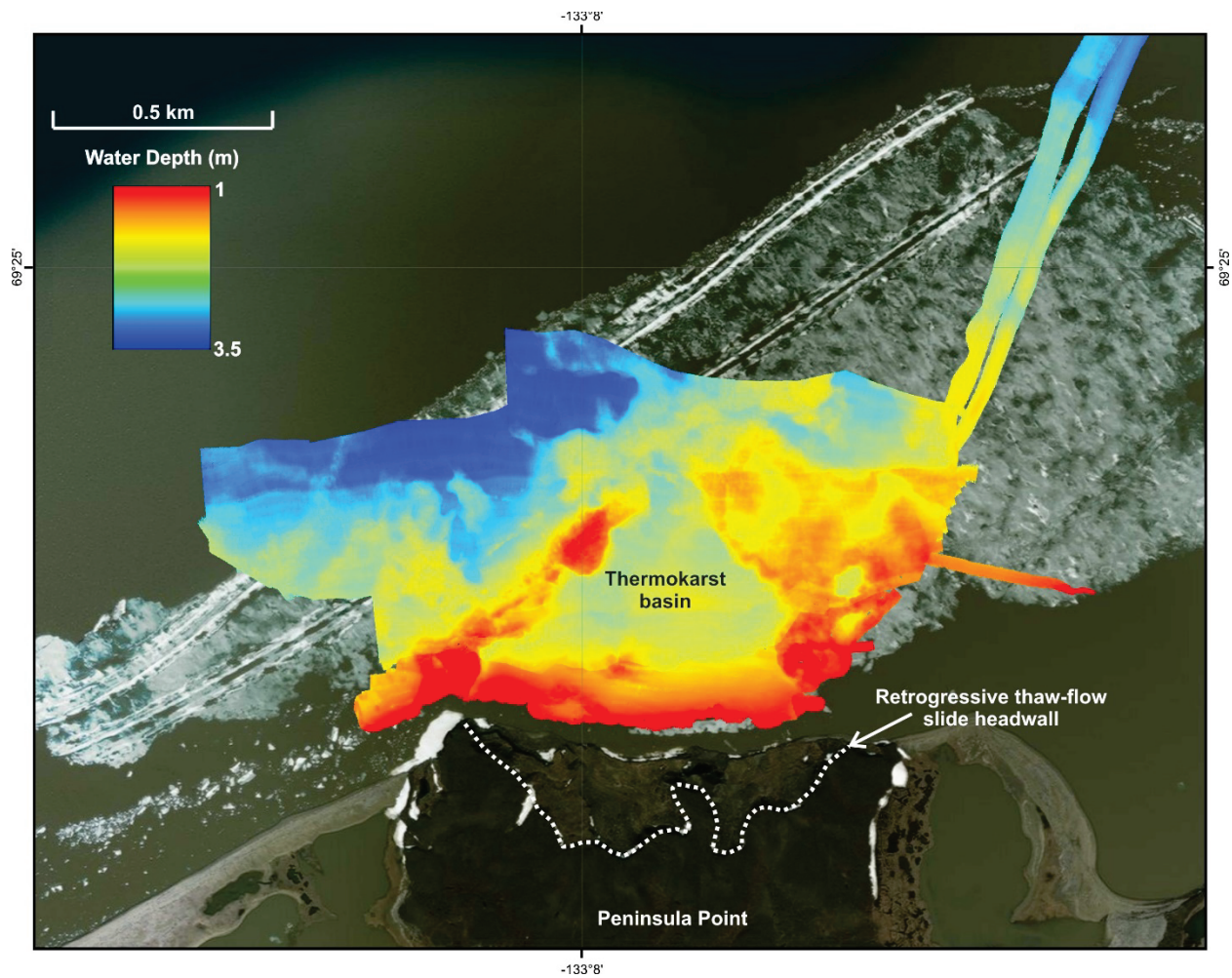
Figure 6: Multibeam bathymetry of area offshore of Peninsula Point.

Acknowledgements

References

Johnson, K., Solomon, S., Berry, D., and Graham, P. 2003. Erosion progression and adaptation strategy in a northern coastal community. M. Phillips, S.M. Springman, L.U. Arenson (Eds.), Final Proceedings, 8th International Conference on Permafrost, Zurich, Switzerland, July 20–25, 2003, International Permafrost Association, pp. 489-494.

Mackay, J.R. and Dallimore, S.R. 1992. Massive ice of the Tuktoyaktuk area, western Arctic coast, Canada. Canadian Journal of Earth Science, **29**: 1235-1249.

CHAPTER 3 – Acoustic mapping of lakes along the Inuvik-Tuktoyaktuk Highway

Kampmeier, M., Weiss, T. and Greinert, J.

Objectives

Thawing permafrost can lead to dramatic loss of sediment strength, sediment consolidation and surface stability. In some cases, especially adjacent to lake shores, slumping or retrogressive thaw flow slides can occur. The objective of the study was to locate and investigate short term permafrost thaw events, where rapid sedimentation is occurring and methane could be released. Field work included mapping the lake bottom morphology and determining the extent of underwater slumps. These data guided the selection of water sampling locations and atmospheric methane surveys. Our goals with the lake surveys were also to demonstrate an approach to lake characterization using light weight equipment that can be rapidly deployed by a small research team. It is our hope is that these data can be used as a basis for monitoring changes and long-term trends.

Methodology and Fieldwork Summary

Field work was conducted with a collapsible canoe equipped with GARMIN GPS and two sonars: A PanOptix Multibeam PS30 with a frequency of 417 kHz and a GT52HW-TM single beam with CHIRP technology (260/455/800 kHz) for creating depth profiles of the lakes. We did not detect any acoustic evidence of gas releases in any of the lakes from the sonar data.

Preliminary Results

In general, we found it challenging to locate candidate study lakes that were suitable to reach with the canoe and that had an active thaw slump along the shore of the lake. While the equipment we utilized functioned effectively without helicopter support, considerable physical effort was involved. We chose three lakes for mapping, arbitrarily named Lake 3, Lake 6 and Lake 9.
Lake 3 was approximately 6000 m^2 in area with a small active thaw slump occurring on the southwestern shore (Fig. 7). The eastern lake bottom was generally less than 2 m deep and quite flat. A small mini basin to 2.5 m deep was located adjacent to the thaw slump in the western part of the lake.

Figure 7: This map shows 'Lake 3', next to the Inuvik-Tuktoyaktuk Highway. The position of water (blue), CTD (circle with point) and air sampling locations (white) are marked.

Lake 6 (3.1 km^2) is much larger than Lake 3 (0.015 km^2) with two small thaw slumps located on the northern shore of the lake. The bathymetry of the lake bottom was variable, with water depths less than 2 m in the eastern and southern parts of the lake. The western part of the lake had a distinct basin that was 8 m deep. Only the most easterly slump area showed a slight change in bathymetry that was possibly coincident with the slump (Fig. 8).
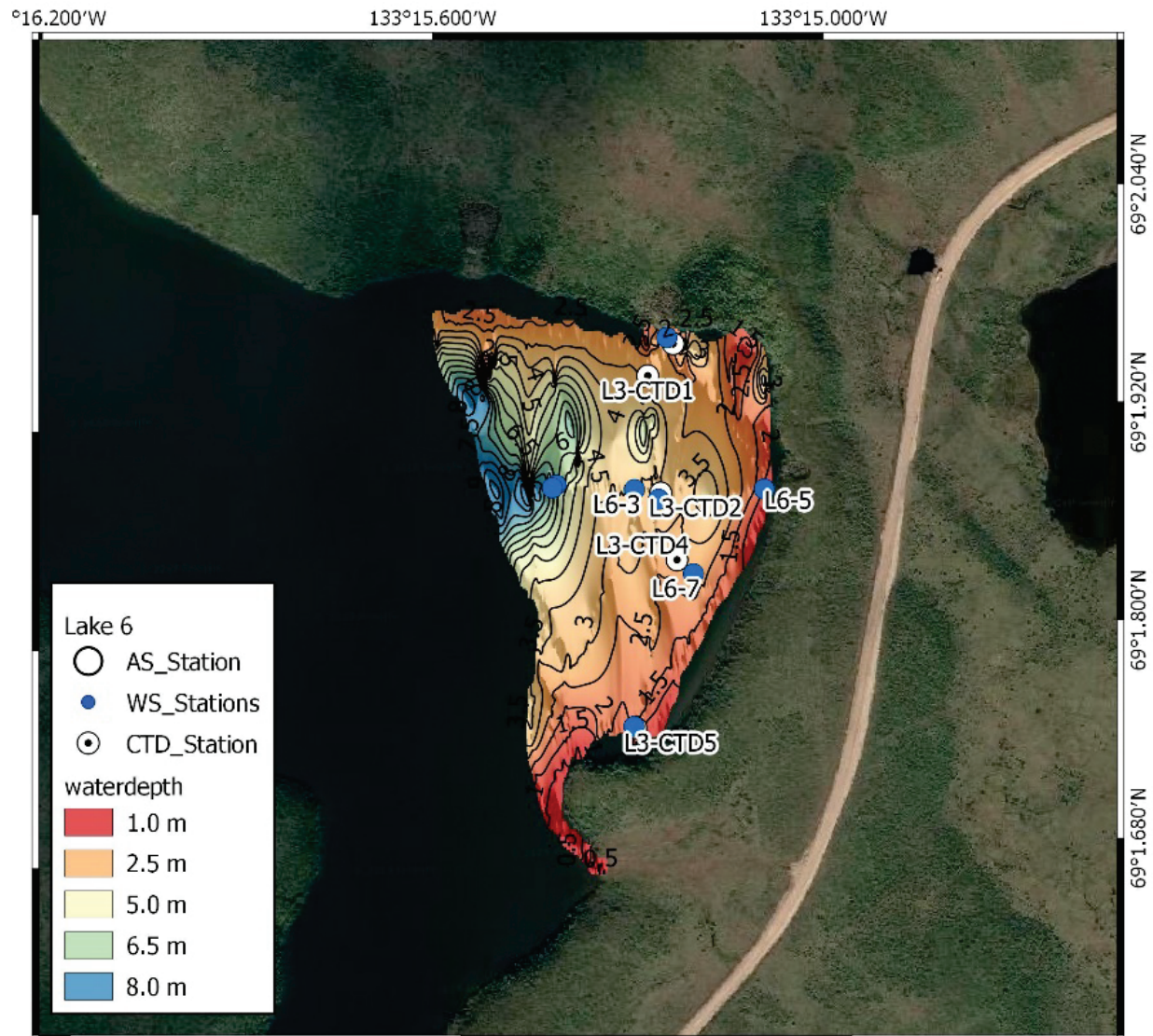
Figure 8: This map shows 'Lake 6', next to the Inuvik-Tuktoyaktuk Highway. The position of water (blue) and CTD stations (circle with point) are marked.

Lake 9 (Fig. 9; 0.065 km²) had an active thaw slump on the southeast shore. A very small mini basin 5 m deep occurred immediately offshore of the thaw slump (Fig. 9). The lake morphology is characterized by three basins, whereby the central basin is the deepest and has a relatively steep slope. Figure 10 shows a thaw slump on the southern shore of 'Lake 9'.
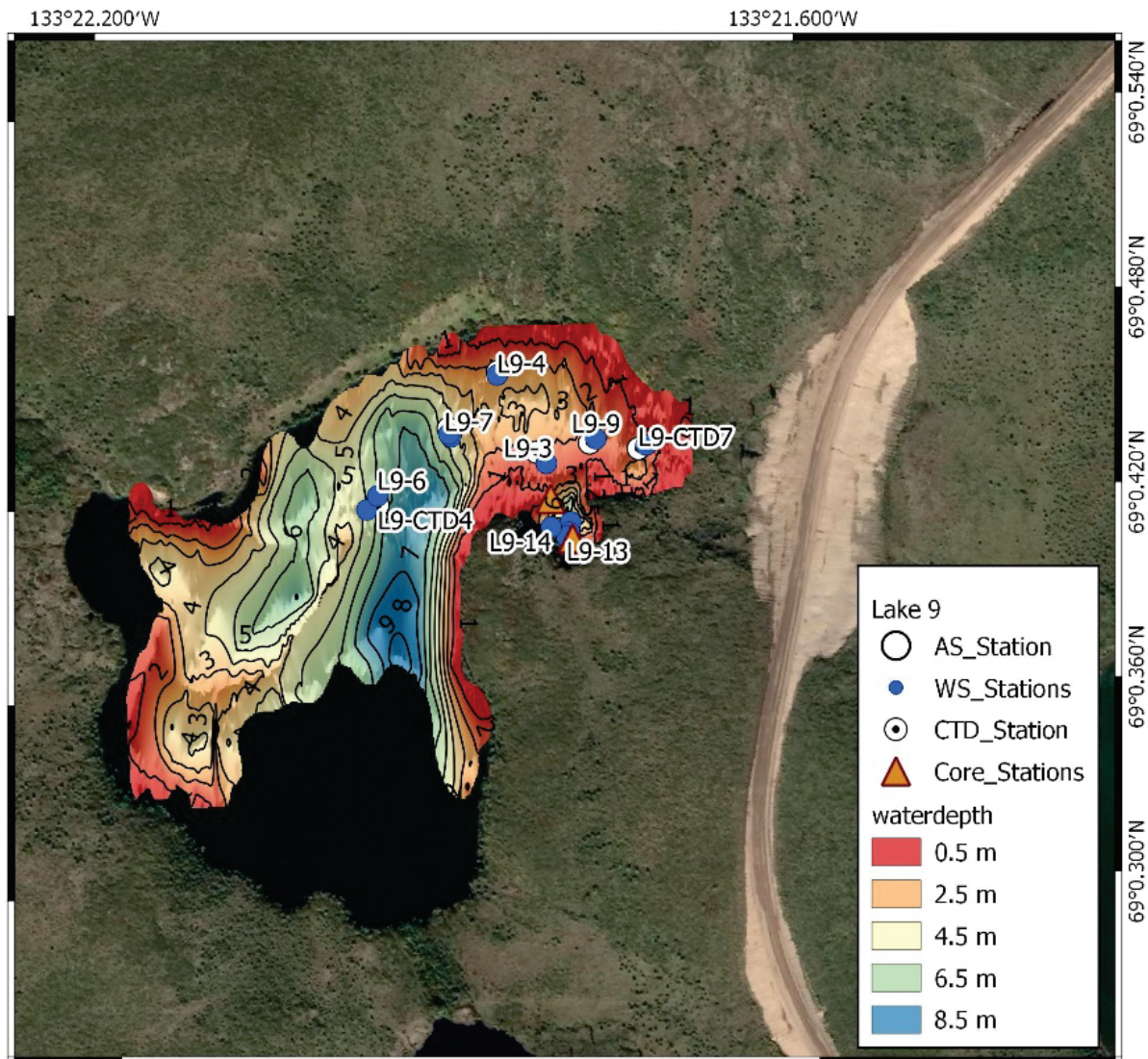
Figure 9: This map shows 'Lake 9', next to the Tuktoyaktuk-Inuvik Highway. The position of water (blue), CTD (circle with point) and air samples (white) are marked. Furthermore, two sediment cores were taken.

Figure 10: A ca 40 m wide and up to 12 m high thaw slump extends on the southern shore of 'Lake 9'. Multibeam mapping revealed that the slump continues underwater to 8 m water depth at about 50 m distance.

CHAPTER 4 – Carbon geochemistry in lakes and coastal erosion sites

Nehir, M., Achterberg, P.E., Bussmann, I. and Overduin, P.P.

Objectives

Permafrost processes like thawing slumps and coastal erosion accelerate enormous amount of carbon release in the Arctic in response to climate change (Grosse et al., 2013; Miller et al., 2014). The scientific objective of our field work was collecting and analyzing the dissolved carbon data from the lakes and coastal waters that is required to understand the carbonate system changes in the Arctic.

Methodology
Total Alkalinity and Dissolved Inorganic Carbon Sampling

Water samples for Total Alkalinity and Dissolved Inorganic Carbon (TA/DIC) were drawn in the laboratory directly from 2 L Nalgene bottles that were taken at different depths from undisturbed sites in lakes or coastal sites. The samples were filtered through a pre-rinsed Pall AcroPak 1000 Supor Membrane 0.8/0.2 µm filter. The filtered water sample was filled into 250 ml Pyrex borosilicate glass bottles. One end of silicone tubing from the filter was placed to the bottom of the glass bottle and the bottle was rotated while filling to ensure no bubbles accumulate inside, overflowing was allowed to avoid the persistence of any minute bubbles. Samples were preserved by adding 100 µl of 50% saturated $HgCl_2$ solution after removing 2.5 ml of sampled water for headspace (Dickson et al., 2007). A thin layer of silicone grease was applied around the glass stoppers and following appropriate labelling, the bottles were sealed and stored in the dark for later analysis at GEOMAR. Analysis will be performed using a conventional titration method for TA measurements and coulometric titration for DIC measurements on a SOMMA (Marianda) analyzer. Water sampling lists for TA and DIC at the lakes and coastal erosion sites include the sample label, date, latitude, longitude, notes and water depth (see Appendix A- Tables 7 – 11).

Preliminary Results

We investigated three lakes (Lake 3, Lake 6 and Lake 9, Tables 7, 8 and 9). At the coast we focused on two erosion sites (Tuk-Peninsula and Tuk-Island, Tables 10 and 11), and a more protected site in Tuk-Harbour (Table 12). Sampling in the estuary of the Mackenzie River as well as the river itself is shown in Tables 13 and 14. All samples were shipped to the home laboratory and will be analyzed upon arrival.

References

Dickson, A.G., Sabine, C L., and Christian, J.R. 2007. Guide to best practices for ocean CO_2 measurements. PICES Special Publication 3.

Grosse, G., Jones, B., and Arp, C. 2013. Thermokarst lakes, drainage, and drained basins. *In* Treatise on Geomorphology. *Edited by* J. Shroder, R. Giardino, and J. Harbor. Elsevier. 29 p. doi:10.1016/B978-0-12-374739-6.00216-5.

Miller, L.A., Macdonald, R.W., McLaughlin, F., Mucci, A., Yamamoto-Kawai, M., Giesbrecht, K.E., and Williams, W.J. 2014. Changes in the marine carbonate system of the western Arctic: Patterns in a rescued data set. Polar Research, **33**(1): 20577. doi:10.3402/polar.v33.20577.

CHAPTER 5 – Nutrients and further geochemistry of lakes and coastal erosion sites

Bussmann, I., Nehir, M. and Overduin, P.P.

Objective

The objective of this study is to obtain more detailed information on nutrient concentrations, hydrography and stable isotopes of the water column to better understand the geochemistry of the selected lakes.

Methodology

Water samples were taken at the surface and the bottom in transects crossing the lake or coastal site from locations with observed erosion to presumably undisturbed locations. A conductivity/temperature/depth (CTD) profile (Seacast CTD, Version 4.4.0) was taken at each site prior to water sampling. The CTD, as well as the water sampler (1.5 L Uwitec, Austria), were attached to a marked rope and lowered by hand. Water samples were transferred to 2 L Nalgene bottles and processed in the laboratory.

Water samples for dissolved organic carbon (DOC) and colored dissolved organic matter (cDOM) were filtered through a pre-rinsed disposable GF/F syringe with a pre-filter 0.7 μm pore size. 20 ml of filtrate was placed into a glass vial and 25 μl of 30 % HCl was added for conservation. About 40 ml of filtrate was filled into dark glass bottles and placed in cool storage. Samples were also collected for the analyses of stable isotopes of water (unfiltered, 30 ml), major cations/total elements (15 ml, filtered through 0.45 μm pore size cellulose acetate filters and conserved with 65% HNO_3), major anions (8 ml, filtered through 0.45 μm pore size cellulose acetate filters). Oxygen, pH and conductivity were measured in the laboratory with a WTW 340i Multiprobe. Before each measurement the sensor was calibrated for oxygen and pH (see Tables 7-14).

Inorganic Nutrient Sampling

Water samples for inorganic nutrients (nitrate/nitrite, phosphate and silicate) were taken from 2 L Nalgene bottles in the laboratory within a few hours of sampling. During sampling, latex gloves were worn to avoid contamination. A pre-rinsed Pall AcroPak 1000 Supor Membrane 0.8/0.2 μm filter (with pre-filter) was used to transfer samples into acid washed (10% HCl) 50 ml polypropylene conical centrifuge tubes from Jet Biofil. Samples were preserved with the addition of 100 μl 4M HCl since freezing was not an option. Samples will be analyzed at GEOMAR using a Seal QuAAtro AutoAnalyzer (See Tables 7-14 for preliminary results for nitrate, nitrite, phosphate and silicic acid).

Dissolved Organic Carbon and Dissolved Organic Nutrient Sampling

The water sampling and filtration methods described above for dissolved inorganic nutrients were used for collecting samples of DOC and dissolved organic nitrogen (DON). The filtered water was collected directly into pre-combusted 30 ml borosilicate glass vials and 100 µl of 4M HCl was added to preserve the samples by lowering the pH of the solution values less than 2. Vials were capped, labelled and stored in the dark. Samples will be analyzed at GEOMAR using a Shimadzu TOC V series analyzer (See Tables 7-14 for preliminary results for DON and DOC).

Preliminary Results

We investigated three lakes (Lake 3, Lake 6 and Lake 9, Tables 7, 8 and 9). At the coast, we focused on two erosion sites (Tuk-Peninsula and Tuk-Island, Tables 10 and 11), and a more protected site in Tuk-Harbour (Table 12). Sampling in the estuary of the Mackenzie River as well as the river itself is shown in Tables 13 and 14.

CTD-profiles revealed no stratification of the water column in all investigated lakes. Temperatures ranged from 8 to 10°C (Fig. 11 for Lake 6). At the coastal sites, we observed a sharp stratification with warm freshwater at the surface and colder saline water at the bottom (T < 8°C, PSU around 10, Fig. 12 for Tuk Island). The stratification was pronounced at the deep (20 m) Tuk Harbour sites with temperatures of 4°C and salinities of >20% (Fig. 13). At these sites the bottom water was also characterized by low oxygen content (2 - 3 mg/l). In the estuary as well as in the river, the water column was well mixed, even at the deep river stations.

Samples for chemistry analyses were shipped to the home laboratory (see Appendix A- Tables 7 - 14).
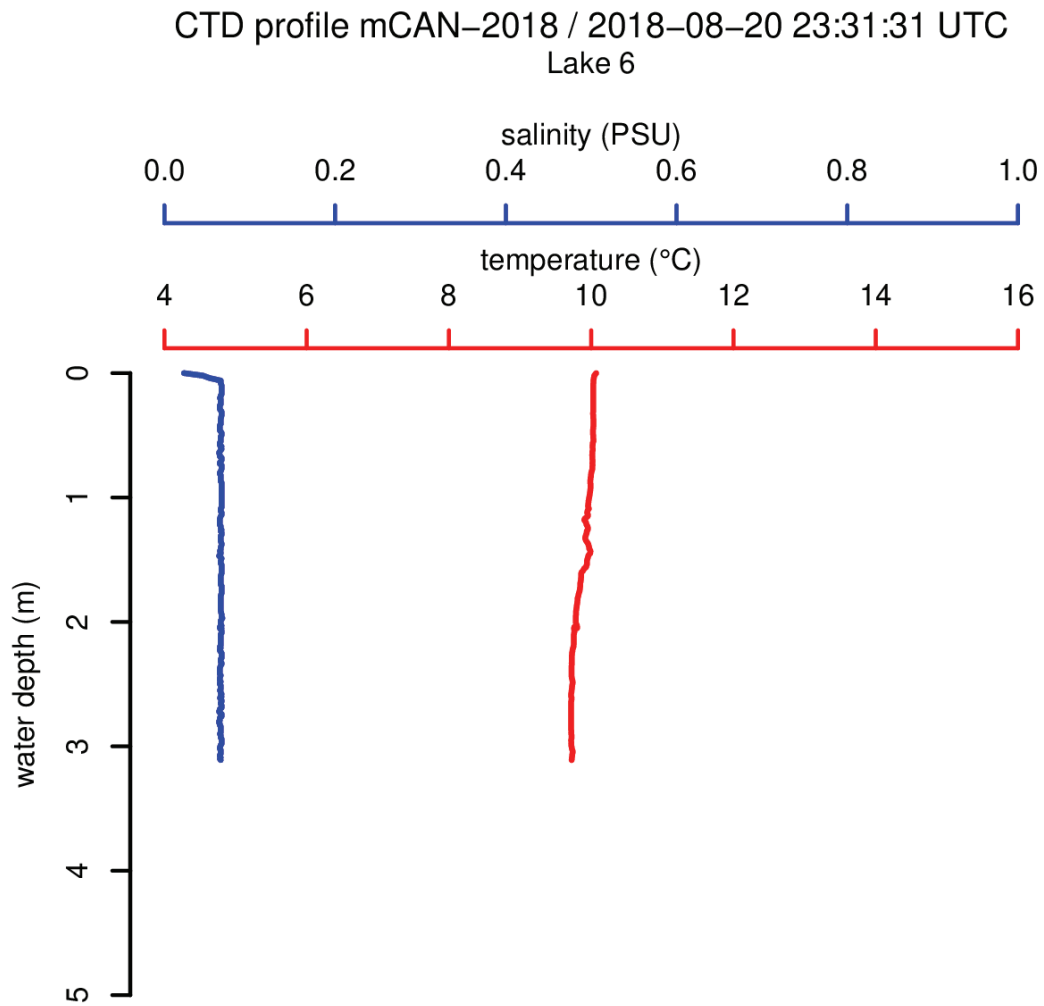
Figure 11: Example of a CTD-Profile at Lake 6.
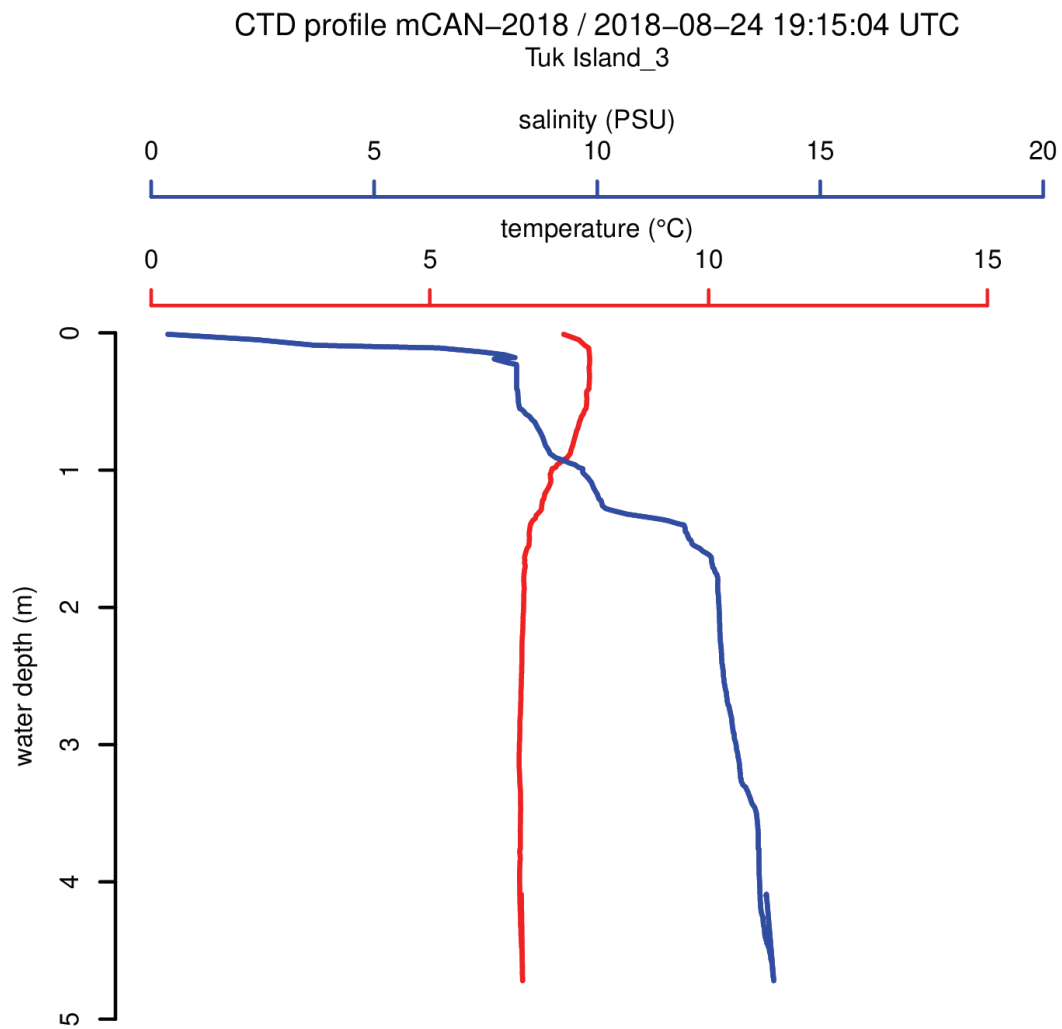
Figure 12: Example of a CTD-Profile at "Tuktoyaktuk Island".
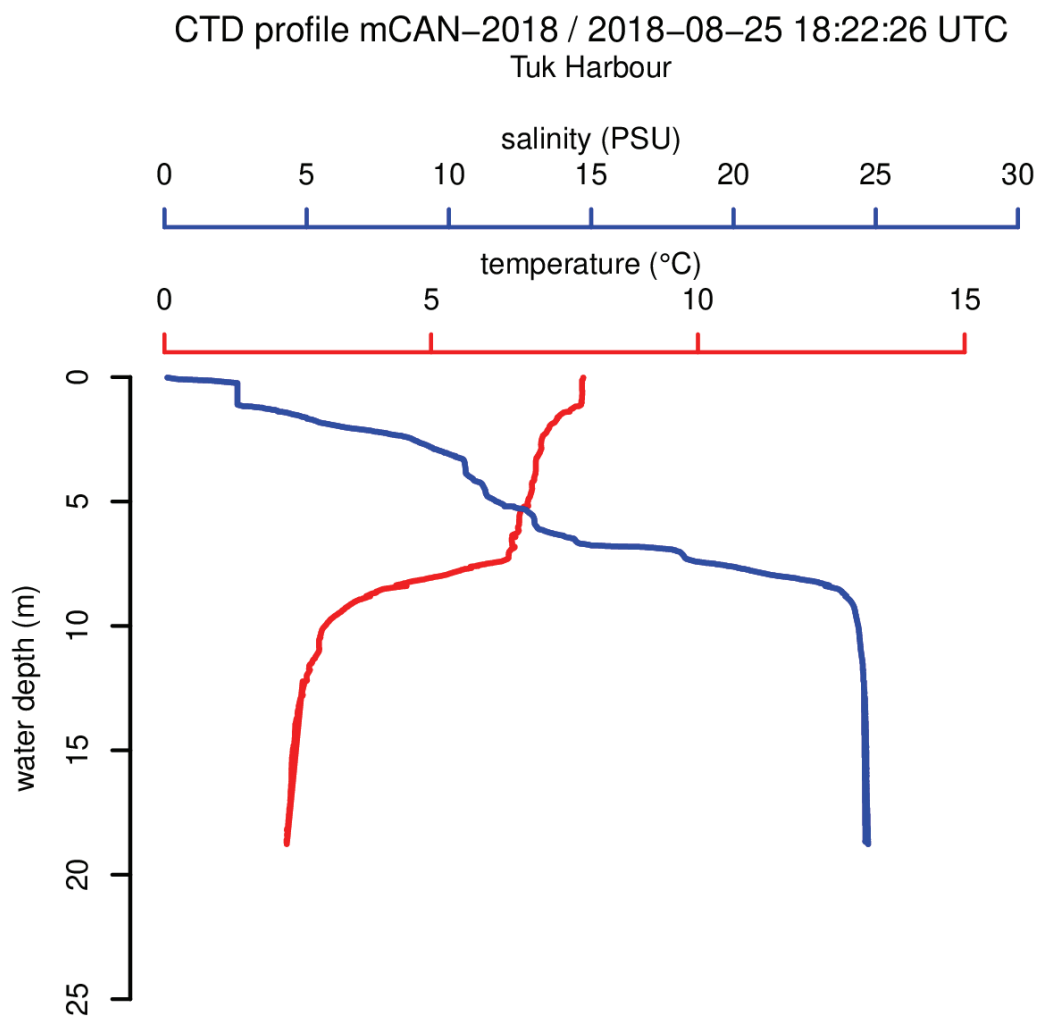
Figure 13: Example of a CTD-Profile from "Tuktoyaktuk Harbour".

CHAPTER 6 – Methane concentrations within sediments, water and air at locations in the Mackenzie Delta and Tuktoyaktuk Peninsula

Bussmann, I., Kampmeier, M. and Weiss, T.

Objectives

Thawing permafrost can, under some circumstances, release methane gas into the surrounding atmosphere. One objective of our field program was to evaluate new technologies to detect methane release that could result from local thaw events or natural geologic processes. Our strategy was to document methane concentrations within sediments, water and air as a basis to consider how much of the released gas reaches the atmosphere.

Methodology and Fieldwork Summary

Methane concentrations in the water were determined with the headspace method (Magen et al. 2014), as well as with the continuous degassing and subsequent detection with a portable Greenhouse Gas Analyzer (Dissolved Gas Extraction Unit and Ultraportable Greenhouse Gas Analyzer, both Los Gatos Research).

Water sampling followed the scheme of water chemistry (see Section 2.3, Tables 7 to 14). At the coastal sites, 120 ml glass bottles were filled without bubbles and capped with butyl septa and aluminum crimps. After adding 10 ml of synthetic air (Alphagaz 1), we added 0.2 ml of 8 M NaOH. For the lakes, 60 ml syringes were filled with 40 ml of water and 20 ml of air. After shaking for 2 minutes, 10 ml of the headspace (containing the methane) was transferred into 20-ml vials, which had been filled completely with saturated NaCl solution. All samples will be analyzed in the home laboratory.

For in situ measurements of methane a degassing unit of Los Gatos Research was attached to a portable Greenhouse Gas Analyzer (GGA). Both instruments were operated with a car battery. The sample water was sucked in by the internal pump of the degasser either from a bucket with overflowing water from the boat's pump (marine sites) or the inlet was attached to the side of the canoe at approximately 30 cm water depth (lakes).

For later flux calculations, we also need the methane concentration of the air above the water surface. Thus, an air inlet for the GGA was detached from the degasser to allow sampling of the atmosphere. For the marine sites the inlet was fixed to the front boat's rail approximately 1.5 m above the sea, for lakes the inlet was fixed directly to the board of the canoe, approximately 30 cm above the water surface. We also sampled the air along the highway with an inlet fixed to the side

mirror of the car, at a height of approximately 1.70 m above the ground surface. While driving at different dates along the Inuvik-Tuktoyaktuk Highway, air was analyzed directly with the GGA inside the car.

All in situ data were recorded with UTC-time and will be geo-referenced in the home lab with the positioning files.

Sediments samples were taken with a small piston corer, which was released by hand. The sediment was then sampled in different core depths. 3 ml of sediment were added with 1.2 g NaCl + 0.5 ml NaCl solution and stored in 20 ml vials. For the river sediments, we used a small grab sampler for surface samples of methane concentrations, as well as subsamples for porosity and grain size.

Preliminary Results

All methane samples were shipped to the home laboratory and will be analyzed upon arrival. Processing of the in situ methane data are in progress.

We investigated three lakes (Lake 3, Lake 6 and Lake 9, Tables 7, 8 and 9). At the coast, we focused on two erosion sites (Tuk-Peninsula and Tuk-Island, Tables 10 and 11), and a more protected site in Tuk-Harbour (Table 12). Sampling in the estuary of the Mackenzie River as well as the river itself is shown in Tables 13 and 14. The in situ data are published online (see Appendix A- Figure 40 and Table 15).

Methane concentrations above the river water are shown in Figure 14. From Inuvik northwestward along the main channel we observed stable and low methane concentrations above the water surface (< 1.99 ppm). When passing through a very narrow channel with dense reed vegetation at the shore, methane concentrations increased to 2-2.06 ppm methane in the air (see arrows in Fig. 14). During the whole trip we had strong westerly winds. Methane concentrations were also recorded on the trip back to Inuvik on the same route and are being processed.
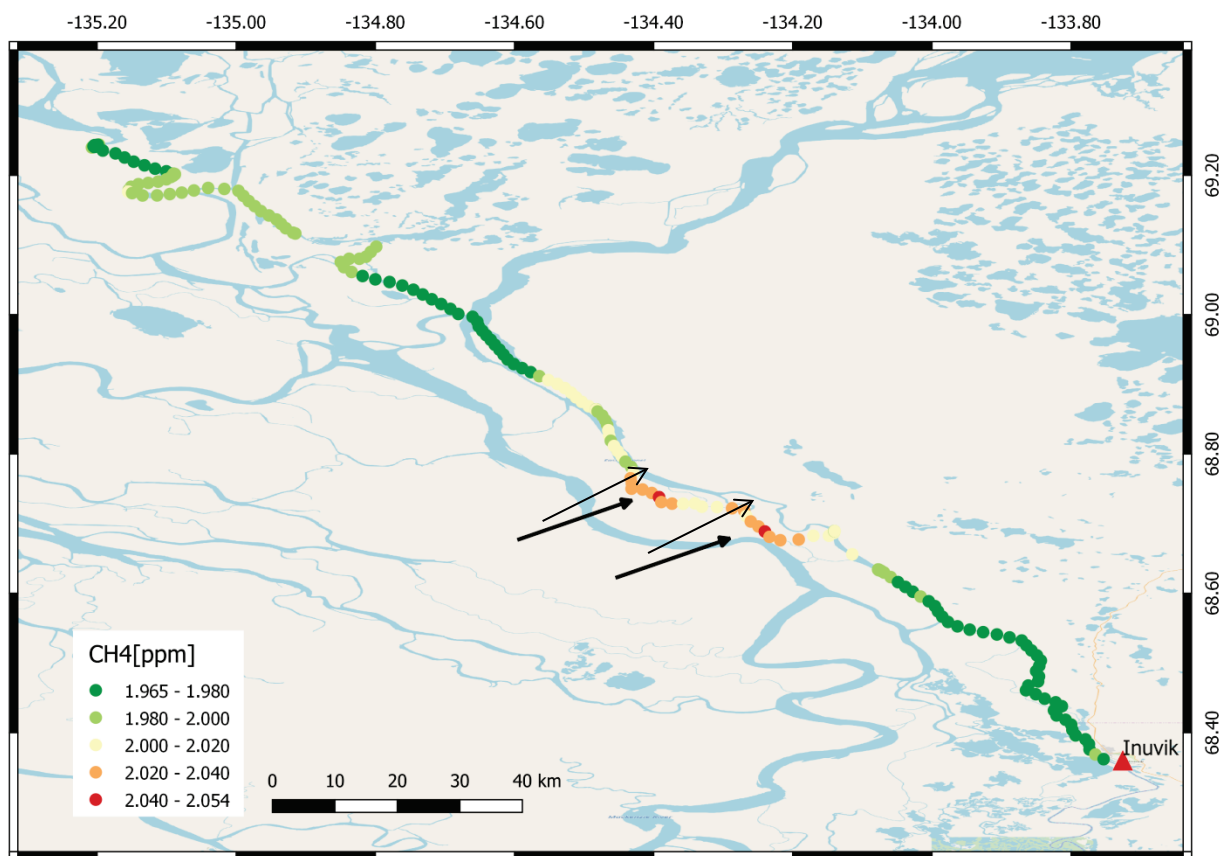
Figure 14: Methane concentration above the water surface along the Mackenzie River on September 03, 2018. Arrows indicate higher methane concentration when passing through a very narrow channel.

References

Magen, C., Lapham, L.L., Pohlman, J.W., Marshall, K., Bosman, S., Casso, M., and Chanton, J.P. 2014. A simple headspace equilibration method for measuring dissolved methane. Limnology and Oceanography: Methods, **12:**637–650.

CHAPTER 7 – Mobile Ocean Bottom Seismometer (MOBSI)

Cable, W., Haberland, C., Ryberg, T. and Overduin, P.P.

Objectives

The spatial distribution of submarine permafrost and its temporal variations are largely unknown. The main aim of this study was to collect ambient seismic noise data at the sea bottom along two transects from the shoreline into the shallow marine area close to Tuktoyaktuk Island, which can be used to estimate the depth to the top of the submarine permafrost layer. Along these profiles, information about the depth to permafrost exists from borehole investigations to which the seismic results can be compared to.

Methodology

MOBSI is a mobile ocean bottom seismometer in a heavy duty pressure housing that is used to record the ambient seismic wave field. The ratio of the frequency spectra of the horizontal to vertical components (H/V) show peak values proportional to the thickness of the unfrozen layer above ice-bonded permafrost, under a set of assumptions regarding the geometry and homogeneity of the sediment below the seabed (Overduin et al., 2015).

For this study, a small boat was used to move into position at each of the measurement points and then anchored to maintain position. The MOBSI, attached to a steel cable outfitted with communications cable, was then lowered to the bottom and allowed to measure the ambient seismic wave filed for approximately 5 minutes. A shipboard monitor allowed the operator to control data quality. The actual data analysis was done in the lab after the measurements.

Preliminary Results

Overall 21 measurements were performed (Fig. 15, Table 1). Preliminary results indicate that the depth to the top of permafrost ranged from approximately 2 m on the beach to approximately 14 m in the shallow marine area (Fig. 16). Highly preliminary interpretations are given in Figures 16 and 17 based on assumed (best-guess) propagation velocities and using an automated peak detection algorithm. Measurements of the depth of the ice-bonded permafrost from two boreholes drilled by the GSC during their spring 2018 nearshore drilling program are also shown (Fig. 15, Table 1). Calibration measurements at locations with known depth to the top of the permafrost layer could be used to determine the propagation velocities above the permafrost, thus further improve the accuracy of the depth measurements.
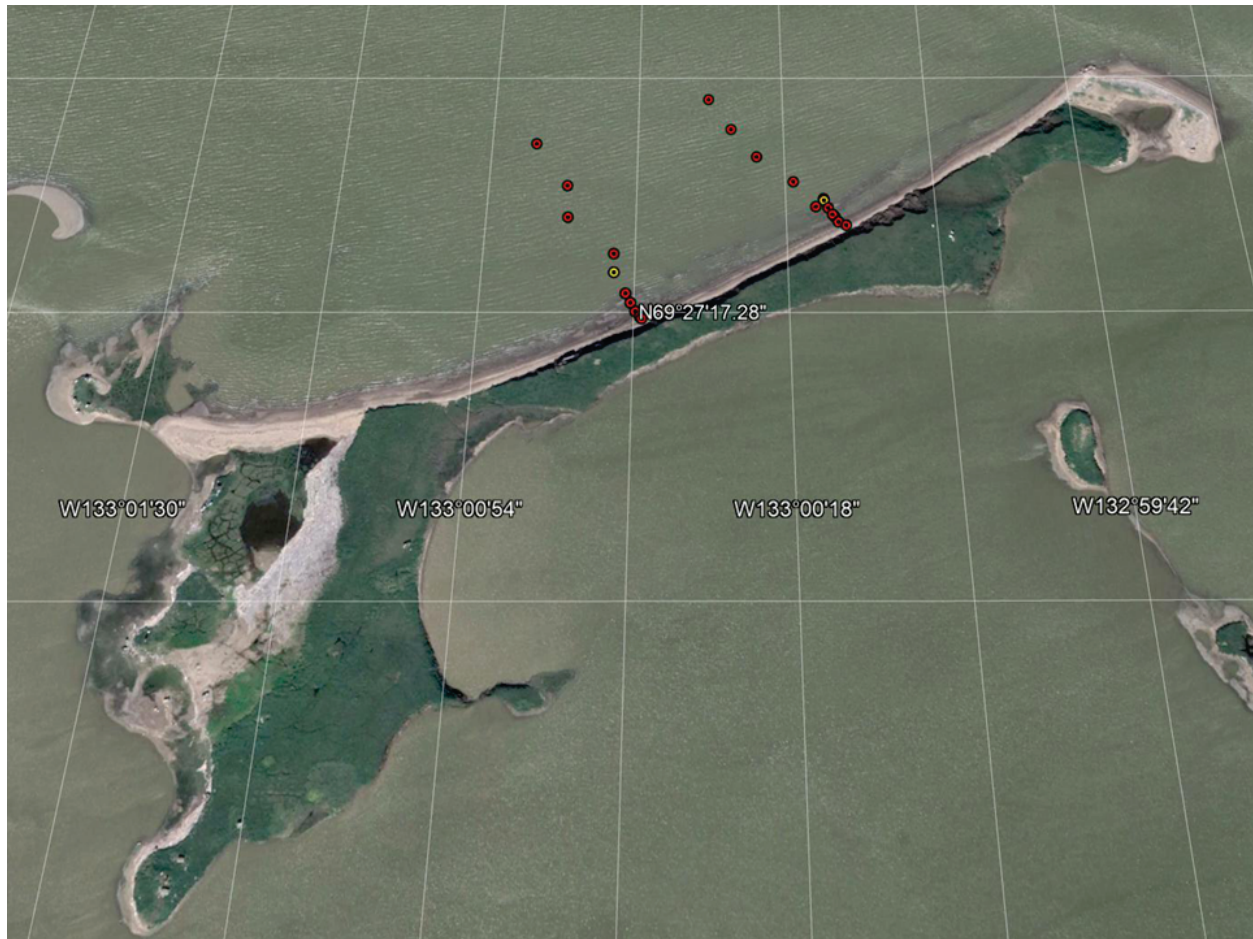
Figure 15: Positions of MOBSI measurements (in red) and the GSC nearshore drilling program borehole sites (in yellow) offshore of Tuktoyaktuk Island are shown. Transect L1 is at right (eastward) and corresponds to Figure 16, while Transect L2 lies westward and corresponds (Fig. 17).

Table 1: Table of the coordinates for all the measurement points with MOBSI.

Sample	Date	Latitude (°N)	Longitude (°W)	Water depth (m)	Notes
2	24.08.2018	69.45797	133.00755	3.83	start transect 1
3	24.08.2018	69.45748	133.00678	3.23	
4	24.08.2018	69.45704	133.00592	3.93	
5	24.08.2018	69.45665	133.00470	1.93	
6	24.08.2018	69.45627	133.00398	0.36	near borehole
7	24.08.2018	69.45639	133.00371	0.51	at borehole 2
8	24.08.2018	69.45625	133.00357	0.46	
9	24.08.2018	69.45615	133.00343	0.15	
10	24.08.2018	69.45611	133.00335	0.00	on beach
11	24.08.2018	69.45604	133.00325	0.00	on beach
12	24.08.2018	69.45599	133.00300	0.00	at bluff base
13	24.08.2018	69.45725	133.01345	4.03	start transect 2
14	24.08.2018	69.45659	133.01231	6.03	
15	24.08.2018	69.45611	133.01224	6.03	
16	24.08.2018	69.45557	133.01067	5.03	
17	24.08.2018	69.45500	133.01025	0.43	
18	24.08.2018	69.45487	133.01008	0.43	
19	24.08.2018	69.45475	133.00992	0.20	
20	24.08.2018	69.45468	133.00977	0.00	on beach
21	24.08.2018	69.45465	133.00971	0.00	at bluff base W
Borehole GSC 2018-2	03.2018	69.4553	133.010646		0-0.9 m: ice 0.9-2.1 m: water 5.2 m: estimated top of permafrost 5.2-14.6 m: ice bonded permafrost
Borehole GSC 2018-4	03.2018	69.456365	133.003697		0-0.9 m: ice in contact with sediment 0.9-2.4 m: estimated top of permafrost 2.4-17.6 m: ice bonded permafrost
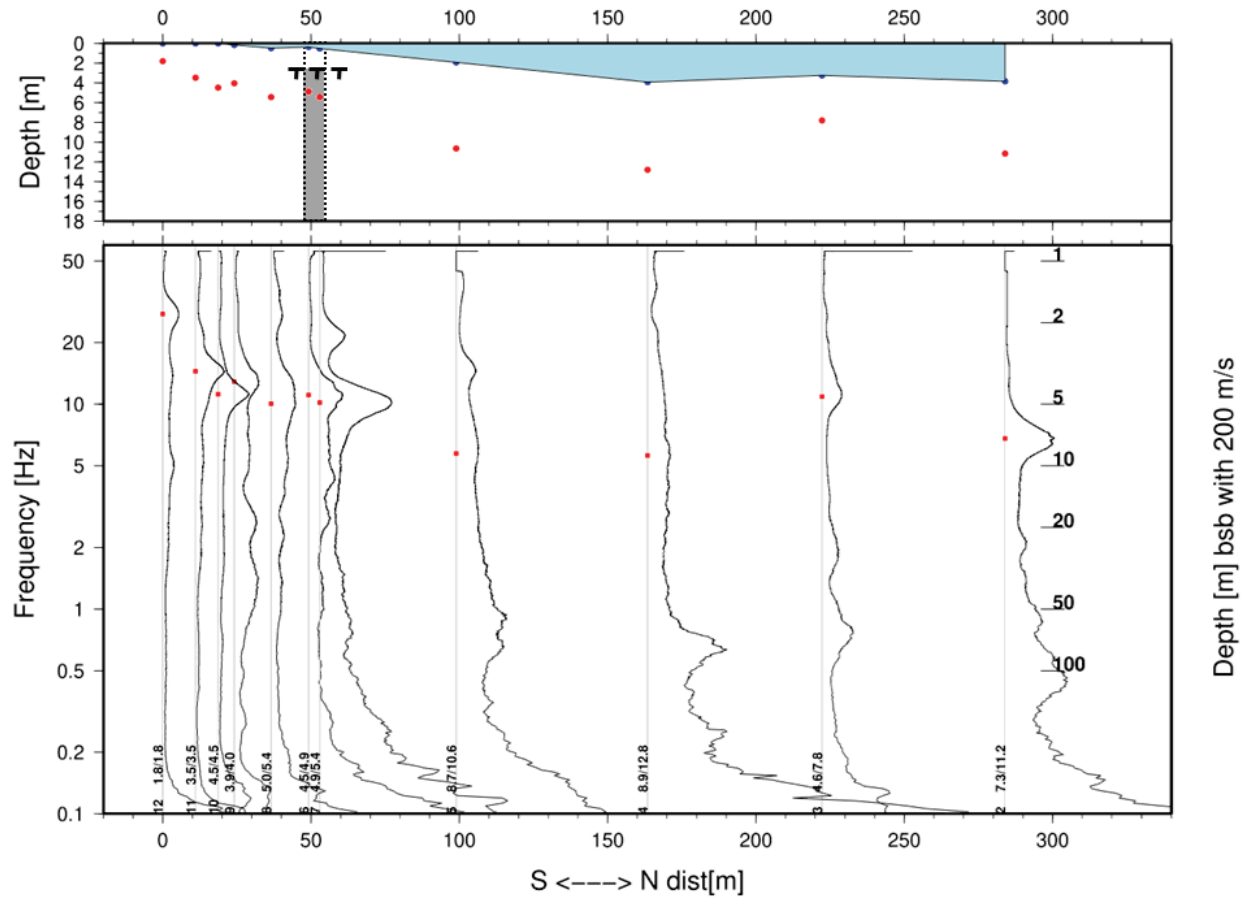
Figure 16: Preliminary results from transect L1 (samples 2-12, see Table 1). Bottom figure shows the horizontal over vertical frequency with the red dots indicating the peak that represents the interface between unfrozen and frozen soil (permafrost). Top figure shows these peaks translated into depths where the red dots indicate the permafrost table and the blue dots indicate the water depth. The position of borehole GSC 2018-2 is indicated, with the ice-bonded permafrost indicated in grey and the permafrost table as a thick dashed line.
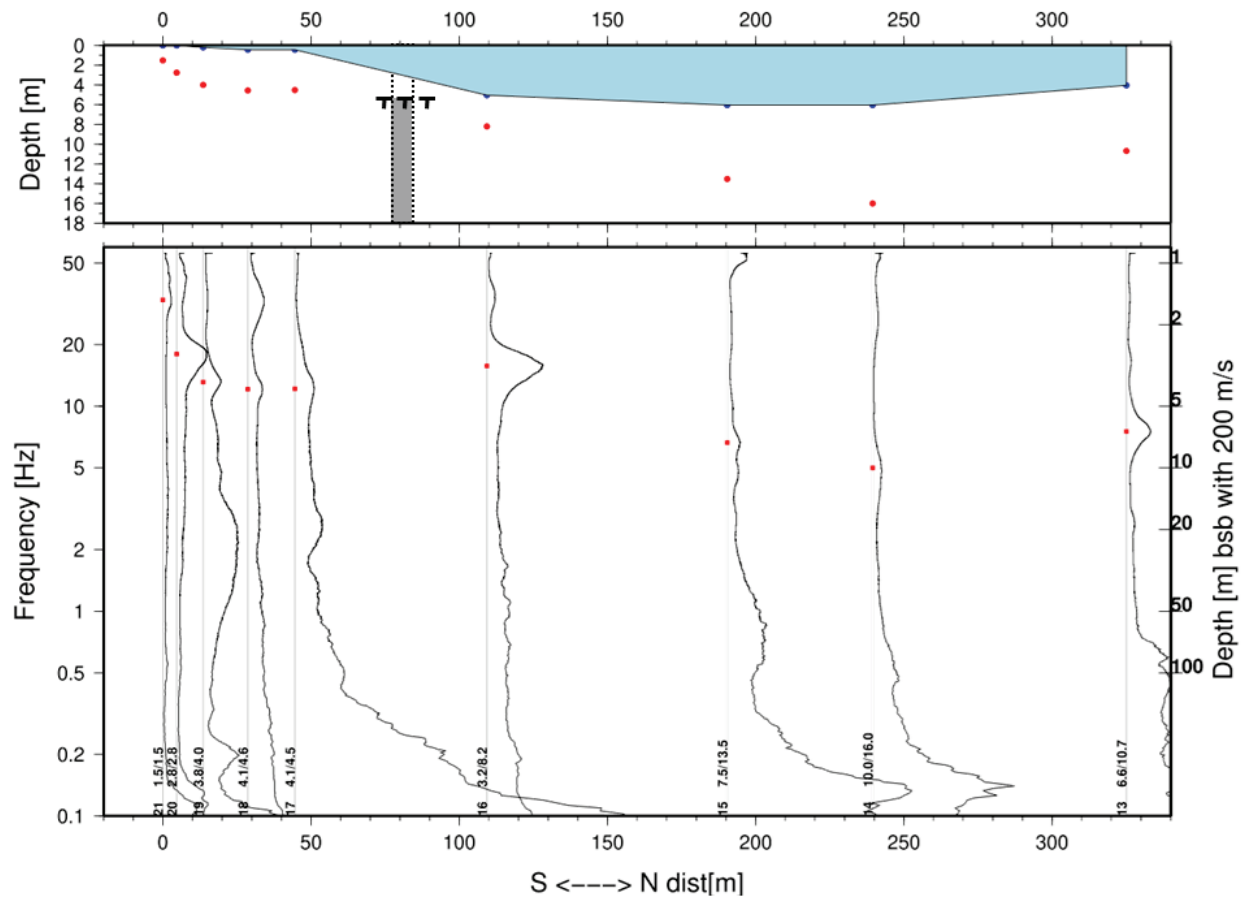
Figure 17: Preliminary results from transect L2 (samples 13-21, see Table 1). The bottom figure shows the horizontal over vertical frequency with the red dots indicating the peak that represents the interface between unfrozen and frozen soil (permafrost). The top figure shows these peaks translated into depths where the red dots indicate the permafrost table and the blue dots indicate the water depth. The position of borehole GSC 2018-4 is indicated, with the ice-bonded permafrost indicated in grey and the permafrost table as a thick dashed line.

References

Overduin, P.P., Haberland, C., Ryberg, T., Kneier, F., Jacobi, T., Grigoriev, M.N., Ohrnberger, M. 2015. Submarine permafrost depth from ambient seismic noise. Geophysical Research Letters, **42**(1):7571-7588. doi:10.1002/2015GL065409.

CHAPTER 8 – Trail Valley Creek Research Station

Boike, J., Lange, S. and Grünberg, I.

Objectives

The PermaSAR project started in 2015 at the Trail Valley Creek Station with the goal to develop a method that improves the detection of vertical movements of the permafrost (heave and subsidence) soil caused by thawing and freezing processes using differential interferometry. Furthermore, the drivers and processes, as well as surface characteristics that affect the subsidence, such as soil and vegetation properties, are investigated. Thus, the field work was continued to maintain the record since the installation of the measurement sites in 2015.

Methodology and Fieldwork Summary

During our field campaign (August 21-27) the following measurements and data were captured:
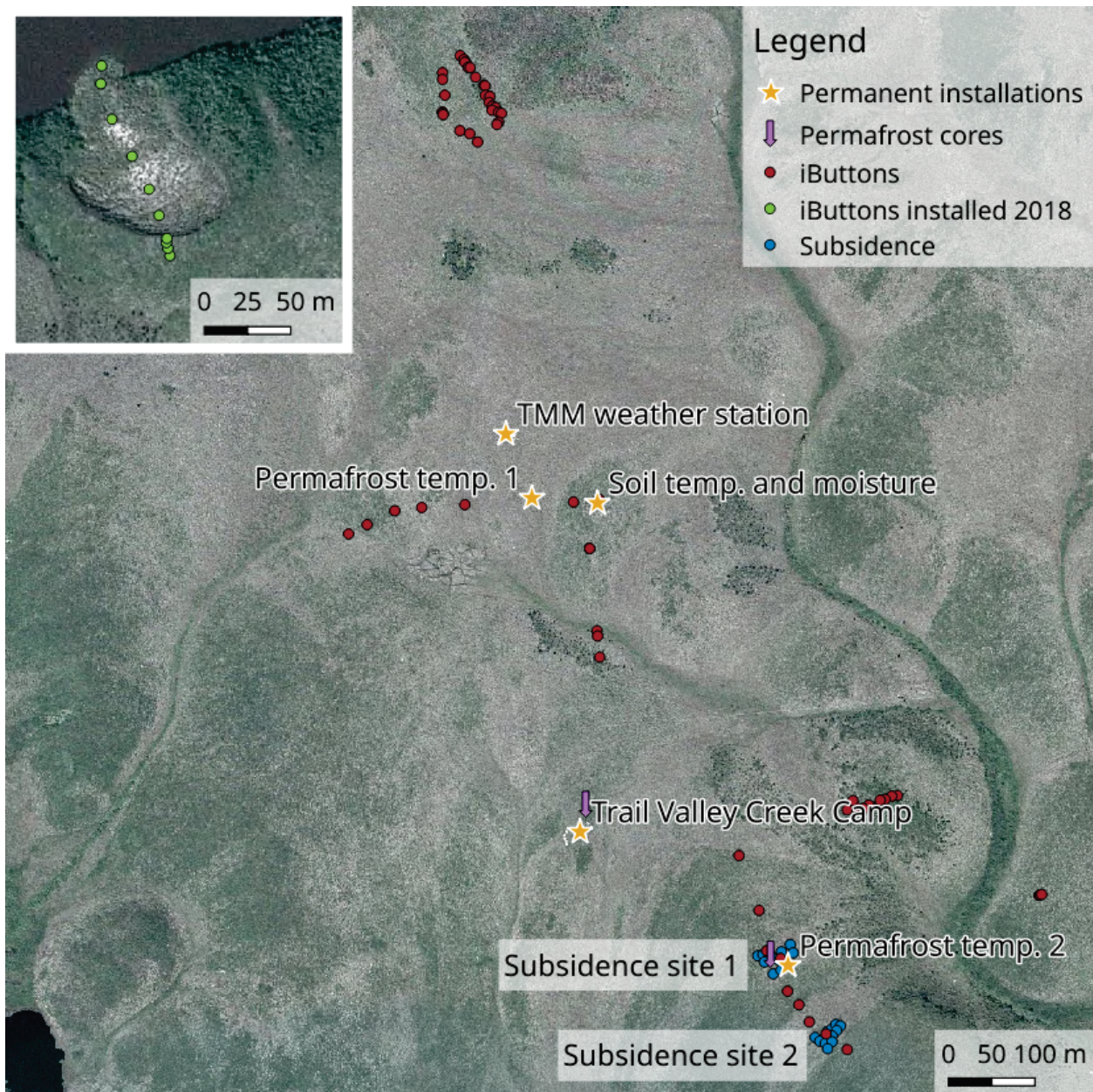
Figure 18: Map of Trail Valley Creek showing the study sites including the distribution of iButtons installed in 2016 (red) and in 2018 (Lake 12, green). Data record is shown in Figure 19. Background map: Mackenzie Valley Orthophoto. Source: NWT Centre for Geomatics.

Figure 19: Subsidence site 1 with the 12 subsidence fiberglass rods (marked with pink flags).

- **Subsidence stations:** At each subsidence station (site 1 and 2, Fig. 19) the visible part of the carbon rods (distance: top of the rods - CD placed on ground surface) was measured five times. The average net subsidence between August 2015 and 2018 for the 24 sites (in total 120 measurements) is 5.2 cm.
- **Active layer (AL) measurements:** The AL was measured at each of the 12 subsidence stations using an AL steel probe (three times around each station). The average AL depth for the 24 sites (in total 72 measurements) is 83 cm (August 22, 2018).
- **GNSS measurements:** Measurement of **subsidence** (x, y, z-coordinates) at the 24 reference rods was repeated with the Leica GNSS system. Additional 16 locations were measured with GNSS at each plot (site 1 and 2) to repeat the survey of August 2016.
- **Permafrost temperature:** The automated temperature sensors (attached to a HOBO U12-008 logger) at site 1 (depths of 4, 20, 117, 217 cm below surface) as well as next to the weather station (site 2: depths of 4, 27, 118, 218 cm below surface) were checked, batteries were replaced and the records were downloaded (Fig. 19).
- **Automated temperature and soil moisture station:** The automated soil temperature and moisture site installed next to the Trail Valley Creek weather station Fig. 19) was read out on August 23, 2018. Dielectric permittivity, soil moisture (Topp et al., 1980) and temperature were successfully recorded hourly at 20 cm, 10 cm, 5 cm and 2 cm depth under the surface (TDR and temp. sensors No. 1, 2, 3, 4). TDR probes 5, 6, 7, 8 were distributed along a horizontal profile as follows: No. 5: next to vertical probes; No. 6: between hummock and shrub-water path; No. 7: inside the shrub water path; No. 8: vertical up for snow TDR. The measuring system consists of a Campbell Scientific CR1000 datalogger, TDR100 Time-Domain Reflectometer, 1x SDMX50 8-Channel 50 Ohm Coaxial Multiplexer, 2x Solar module

and charger, 4xPt100/3 temperature probes, 8x TRD CS630-L probes, Campbell Scientific, UK (rod length 15 cm).

- **iButton temperature sensors** were read out and re-installed just below the surface within 1000 m distance to camp in August 2016 (Fig. 19). For each iButton the GNSS coordinates, the vegetation cover and topography, and active layer thaw depth were recorded. 9 out of the 77 iButtons (ID 11-20) were installed during a helicopter survey in 2016 and were not recovered. 10 additional iButtons were installed at Lake 12 on a transect through the thaw slump. The two-year data series of 68 iButtons reveal systematic differences between the different vegetation types above the sensors. The soil surface temperature below tall shrubs is higher in winter and lower in spring as compared to other vegetation types (Fig. 20).
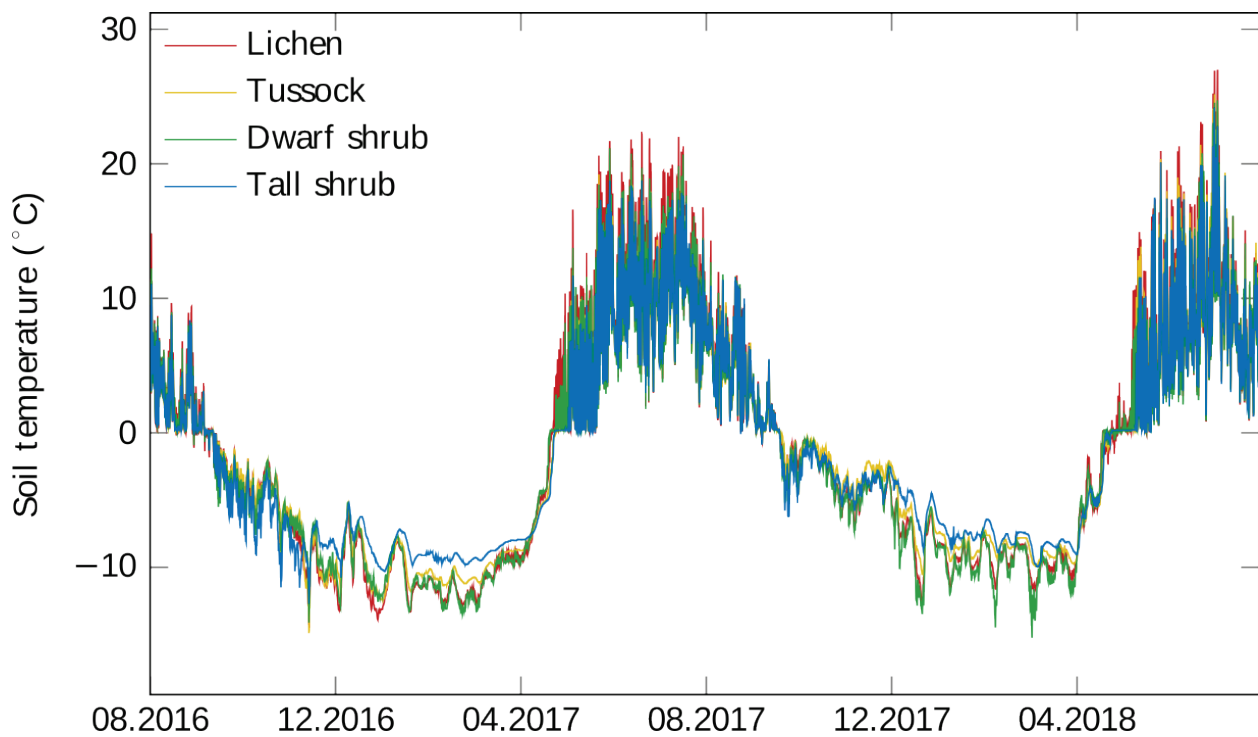
Figure 20: Two years (August 2016 to August 2018) temperature data taken every 3 hours (iButtons). Median values of each vegetation type were calculated from 68 locations. The classification of vegetation was based on field observations and pictures of the iButton locations.

- **Permafrost coring:** A SIPRE (Snow Ice Permafrost Research Establishment; Jon's Machine Shop, Fairbanks, Alaska) coring unit was used to drill into the permafrost at two sites close to camp (Figure 18). First, a hole was dug to maximal active layer thaw depth and samples were taken from the soil profile (Fig. 21). Than the battery powered corer (diameter 5 cm) was used to obtain frozen samples down to a maximum of 37 cm below the frost table (Fig. 22). Due to the occurrence of rocks, drilling was difficult and several attempts were necessary to obtain samples. The soil and permafrost samples were wrapped, kept frozen and transported to Potsdam for analysis of ice content, texture, total organic carbon, carbon/nitrogen/sulfur ratios (C/N/S), biogenic volatile carbon, and microbial communities.

Figure 21: Soil pit down to maximum active layer thaw depth at location Subsidence plot 1 on August 26, 2018. Thaw depth was about 85 cm.

Figure 22: Frozen core (37 cm) retrieved below the maximum active layer thaw depth of 85 cm at subsidence plot 1 (-133.494441, 68.740759) on August 26, 2018 using the SIPRE corer. Samples were wrapped individually and transported frozen to Potsdam in August 2018 for further analysis.

References

Topp, G.C., Davis, J.L., Annan, A.P. 1980. Electromagnetic Determination of Soil Water Content: Measurements in Coaxial Transmission Lines. Water Resources Research, **16**:574–582.

CHAPTER 9 – GPS Interferometric Reflectometry (GPS-IR)

Cable, W. and Boike, J.

Fieldwork Period and location

From August 13 to September 09, 2018, along the Inuvik-Tuktoyaktuk Highway.

Objectives

Our aim was to measure and quantify the amount of ground subsidence due to thawing of ice-rich permafrost; the seasonal heave and subsidence cycle of the active layer; and the accumulation and melting of snow.

Methodology

Instrumentation and Sites

Five sites were instrumented with equipment consisting of a GPS receiver and an Arduino based micro-logger to record raw GPS data from the receiver (Fig. 23). Power to the instrumentation is provided by a deep cycle 12V 79Ah battery and 10W solar panel. With exception of station S006, all sites were equipped with a time-lapse camera programmed to take hourly photos between 10:00 and 18:00 local time, to aid in the interpretation of the data. Two of the sites, S006 and S001 (Table 2 & Fig. 24), were in installed on existing meteorological stations operated by Shawne Kokelj (NWT Department of Environment and Natural Resources). Both of these stations measure snow depth using a sonic distance sensor (SR50, Campbell Scientific); therefore, direct comparisons with the GPS-IR calculated snow depth can be made. However, both stations are resting on the ground surface so they will heave and settle with the seasonal and longer-term subsidence, making it difficult to use these stations for subsidence. The remaining 3 stations (S002, S003, S005) are installed on benchmarks (27 mm diameter steel pipe, Fig. 25) that were installed to a depth of 2.5 to 3 m by Ashley Rudy (Wilfrid Laurier University) to monitor subsidence. Since these benchmarks are well anchored in the permafrost it should be possible to observe the seasonal heave and subsidence cycle along with any subsidence that might occur due to thaw of ice-rich permafrost.

Methodology

This technique, GPS Interferometric Reflectometry (GPS-IR), observes the signal to noise ratio (SNR) of each satellite in view relative to its elevation angle (Fig. 26). The received GPS signal is a combination of the direct and reflected signals. During the overpass of each satellite, the length of the path for the reflected signal changes as the reflection point moves due to the changing elevation angle of the satellite (Fig. 26). This change in path length for the reflected signal causes

the direct and reflected signals to go in and out of phase, which can be observed in the SNR as increasing and decreasing signal strength. Using the SNR and elevation angle the antenna height can be calculated according to:

$$SNR = A(e)sin(4\pi H\lambda^{-1}sin(e) + \phi)$$

Where e is the satellite elevation angle, H is the antenna height above the surface, λ is the GPS wavelength (1.5 GHz) and φ is the phase (Larson, 2016). Daily overpasses from each satellite yield a transect radiating outward from the antenna to a distance of approximately 20 m on which the average height, relative to the antenna, is calculated. As each satellite orbit is different, the azimuth is also different, yielding transects that radiate from the antenna in all directions.

Preliminary Results

The sites have been installed and will continue to collect data for at least one year (Table 2, Figs. 24 and 25). Currently we have only a few days of data to begin working out the processing routine. Once the data has been collected we will begin processing the data to obtain surface height changes through time.

Table 2: GPS-IR site locations and installation dates

Site_ID	Date	Latitude (°N)	Longitude (°W)	Notes
S006	26.08.2018	69.36318	133.03643	Tuk Met Station
S001	29.08.2018	68.53840	133.77406	Inuvik Met station
S002	30.08.2018	69.01260	133.27079	Husky Peatland Sentinal Site
S003	01.09.2018	68.75210	133.54164	TVC Hilltop Sentinal Site
S005	01.09.2018	68.74943	133.54210	TVC Peatland Sentinal Site
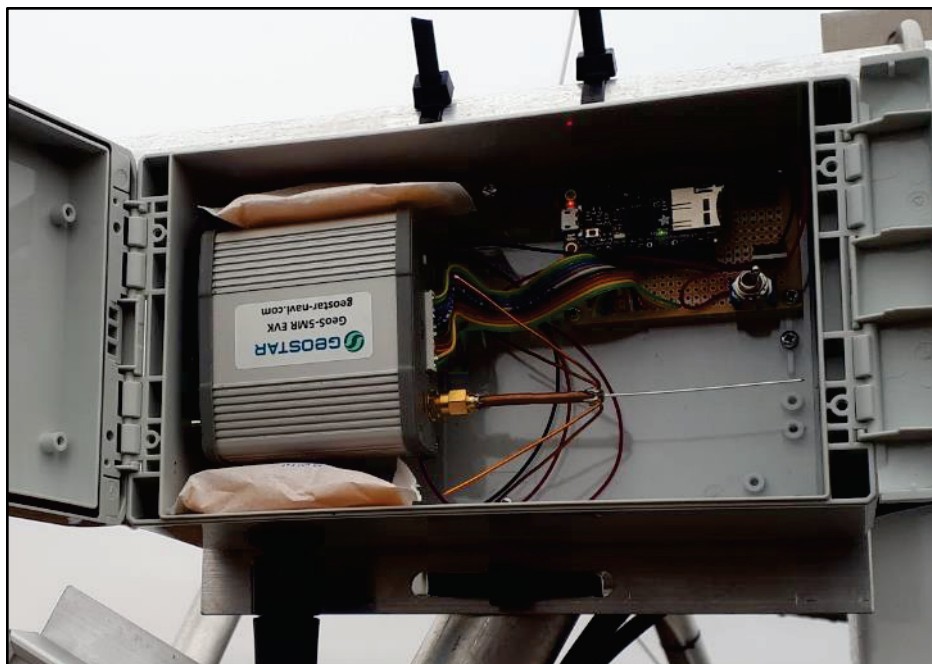
Figure 23: Photo of the GPS-IR instrumentation installed at each site. On the left is the GPS receiver with custom dipole antenna (Chen et al., 2017). On the right is the Arduino based logger for recording the raw GPS data.
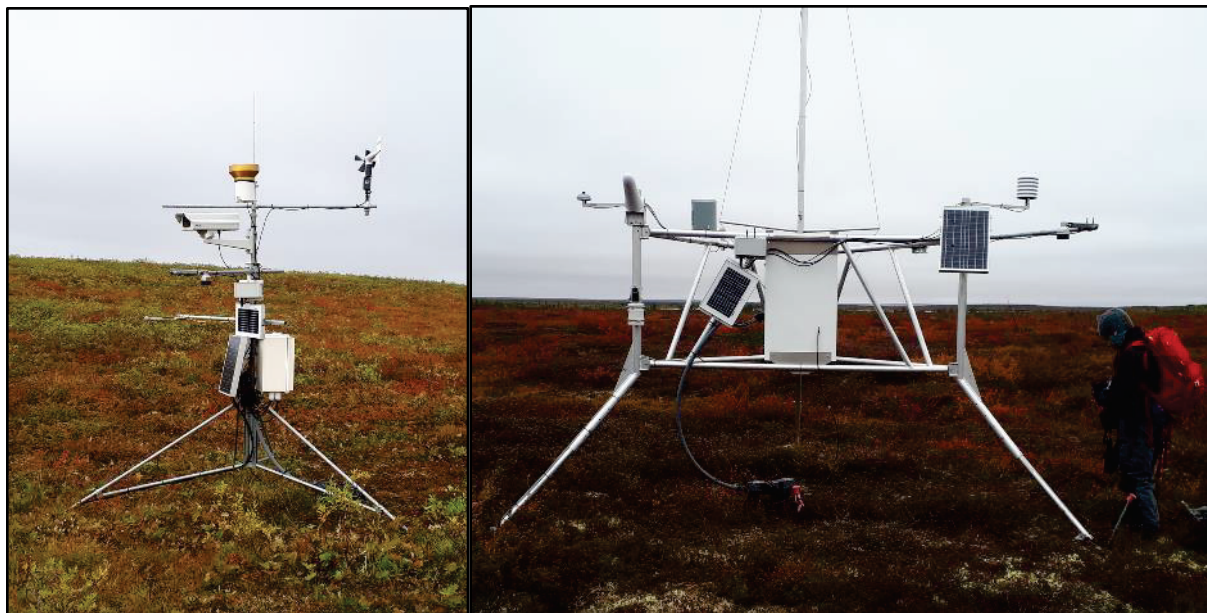
Figure 24: Photos of the GPS-IR instrumentation installed on the two meteorological stations (left: S006 and right: S001).
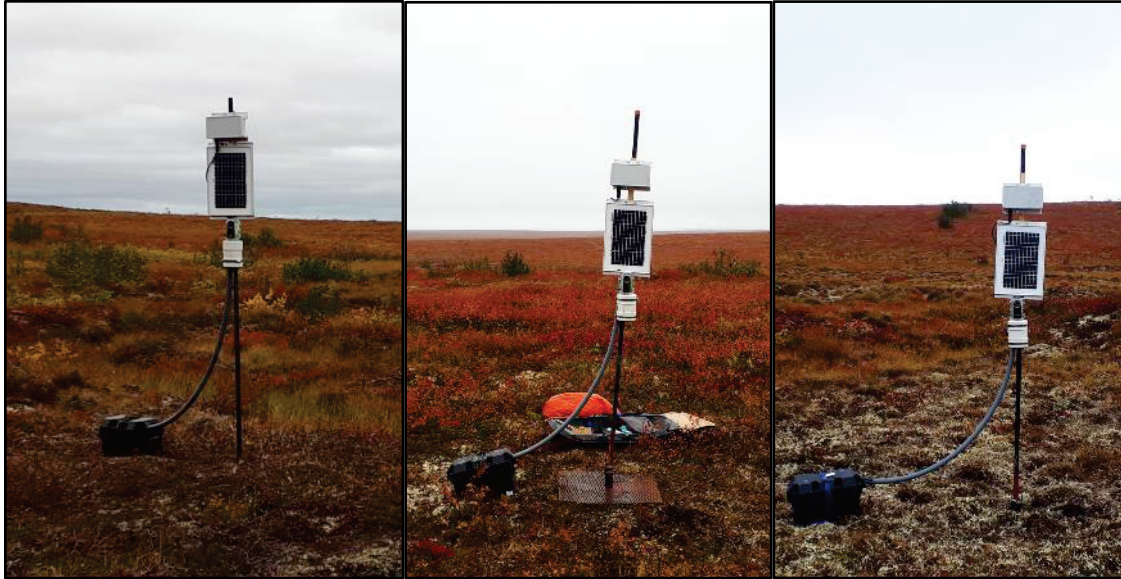
Figure 25: Photos of the GPS-IR instrumentation installed on the benchmarks (left: S002, middle: S003 and right: S005).
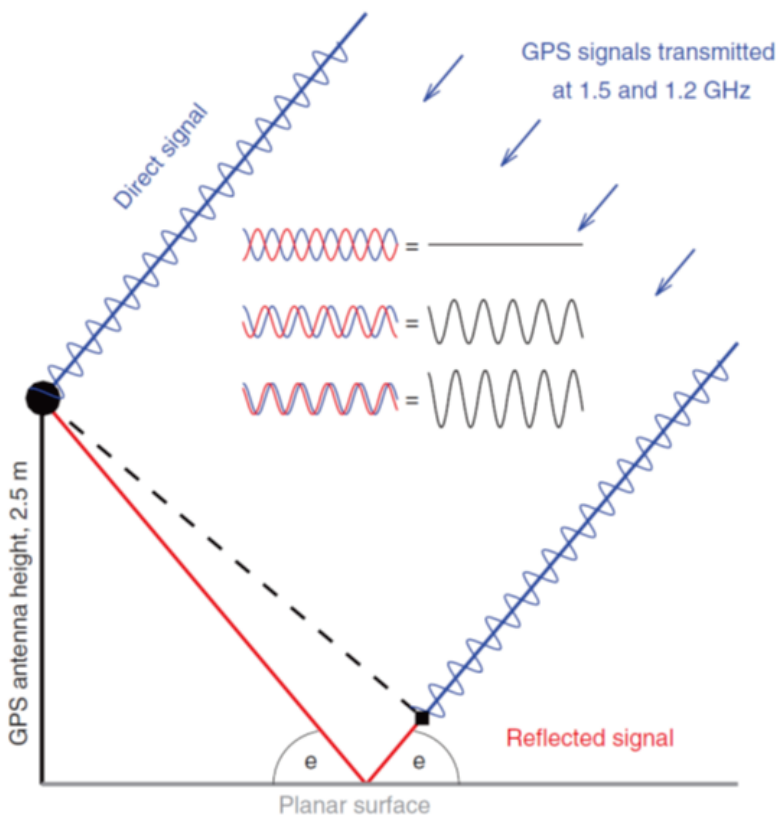
Figure 26: Taken from Larson 2016, this figure shows the path that the direct (blue) and reflected (red) signals take to reach the antenna and how these signals being in or out of phase effects the SNR (black).

References

Chen, Q., Won, D., and Akos, D.M. 2017. Snow depth estimation accuracy using a dual-interface GPS-IR model with experimental results. GPS Solutions, **21**(1):211–223. doi:10.1007/s10291-016-0517-1.

Larson, K.M. 2016. GPS interferometric reflectometry: applications to surface soil moisture, snow depth, and vegetation water content in the western United States. Wiley Interdisciplinary Reviews: Water, **3**(6):775-787. doi:10.1002/wat2.1167.

CHAPTER 10 – Vegetation - permafrost - climate interaction

Grünberg, I., Boike, J., Cable, W. and Lange, S.

Fieldwork Period and Location

From August 18 to September 03, 2018 between the Inuvik-Tuktoyaktuk Highway and the Trail Valley Creek field site.

Objectives

Vegetation alters the surface energy budget and affects radiative fluxes as well as latent and sensible heat fluxes. While we try to cover multiple vegetation types with point measurements (Section 3.4), these measurements are not directly comparable as climate and soil variables depend on weather, time of the day and time of the year. Therefore, we will compare the point measurements with time series measured at two climate stations. The time series will enable us to compare diel cycles and response to weather conditions between four different vegetation types.

Methodology

We set up two automatic climate stations close to each other 170 m to 290 m from the Inuvik-Tuktoyaktuk Highway and 2 km from the Trail Valley Creek field site (Fig. 27, Table 3). The primary climate station recorded the following variables above 30 cm tall dwarf shrub vegetation dominated by *Betula glandulosa* (Fig. 28):

- Wind speed and direction
- Air temperature and relative humidity
- Ground / vegetation surface temperature
- Incoming and reflected shortwave radiation, incoming and outgoing longwave radiation
- Soil heat flux
- Soil moisture at three depths (did not record data)
- Soil temperature at 10 cm, 20 cm, 30 cm, 40 cm, 50 cm, and 60 cm depth

The roving climate station (mobile) was initially set up on dwarf shrub tundra dominated by lichen and different berry shrubs (*Arctostaphylos uva-ursi, Empetrum nigrum*) of approximately 5 cm height. The second location was in a polygonal wetland on a high-centered polygon. The surface was dominated by lichen and dwarf shrubs (*Ledum palustre, Rubus chamaemorus, Arctostaphylos uva-ursi, Vaccinium vitis-idaea*) with some sedges and an average vegetation height of 3 cm above the lichen layer. The third location of the roving station was in low shrub tundra dominated by

Betula glandulosa and *Alnus crispa* with a range of vegetation heights between 50 cm and 2 m. The roving climate station recorded the following variables:

- Ground / vegetation surface temperature
- Reflected shortwave radiation and outgoing longwave radiation
- Transmitted shortwave radiation below canopy
- Soil heat flux

Table 3: Measurement locations of the two climate stations in different periods.

Sample	Date	Latitude (°N)	Longitude (°W)	Notes
Primary climate station	18.08.2018 - 03.09.2018	68.75158	133.54285	Dwarf shrub tundra, *Betula*
Roving climate station, position 1	18.08.2018 - 21.08.2018	68.75211	133.54202	Dwarf shrub tundra, lichen and *Arctostaphylos*
Roving climate station, position 2	21.08.2018 - 27.08.2018	68.74976	133.54064	Dwarf shrub tundra, lichen and *Ledum,* polygonal wetland
Roving climate station, position 3	27.08.2018 - 01.09.2018	68.75093	133.53957	Low shrub tundra, *Betula, Alnus*
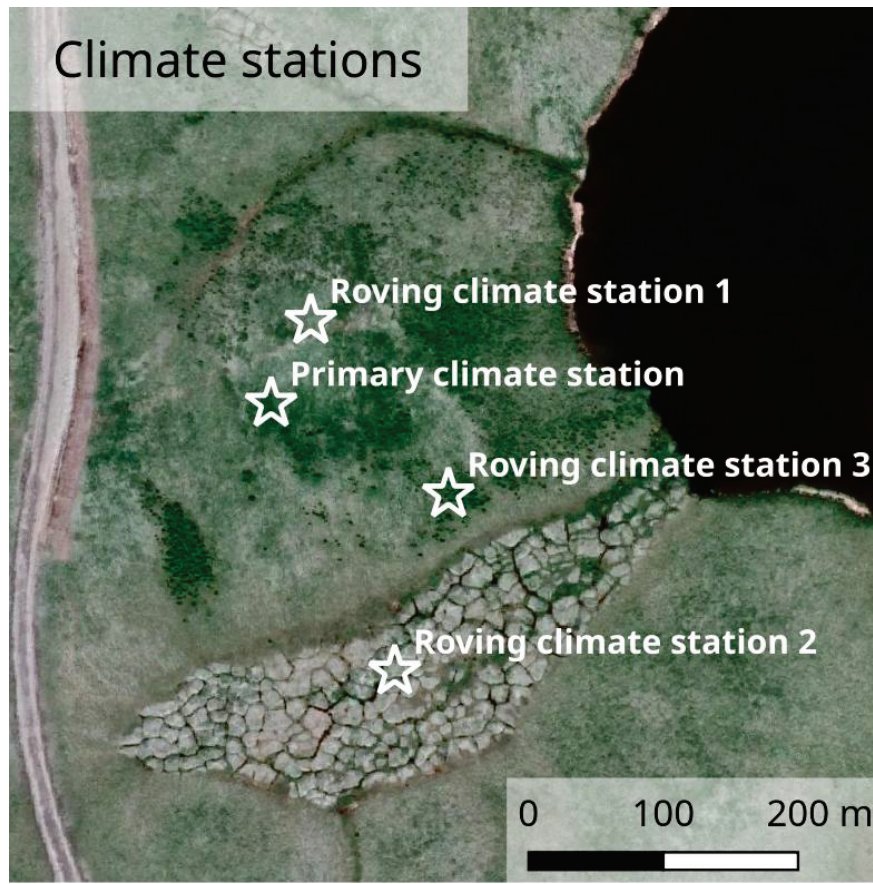
Figure 27: Location of the major climate station and the roving climate station at its three positions close to the Trail Valley Creek field station. Source of background figure: Google satellite.
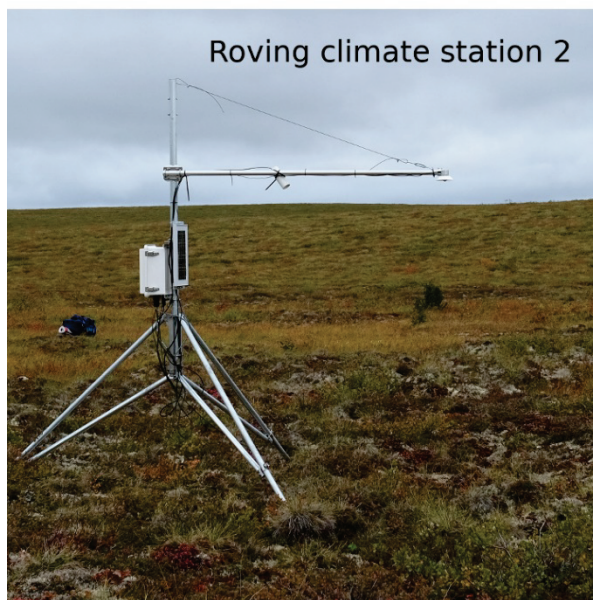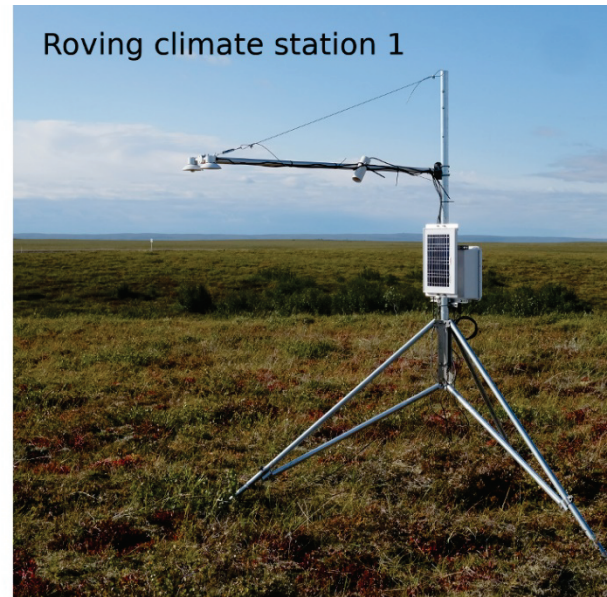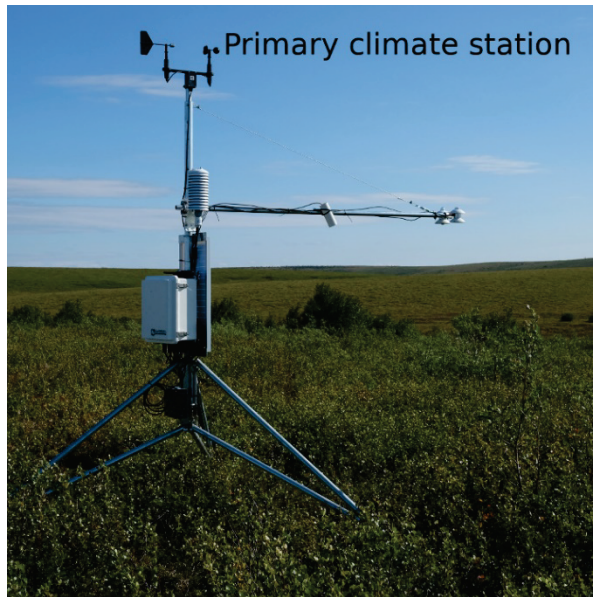
Figure 28: Pictures of the major climate station and the roving climate station at its three positions over different vegetation types.

Preliminary Results

The two automatic climate stations measured energy fluxes, temperatures, relative humidity and wind during approximately two weeks. A first evaluation of the data shows good results for the radiation budget (Fig. 29) and the soil temperature profile below dwarf shrubs (Fig. 30). The soil heat flux at dwarf shrubs is higher than at all other vegetation types (Fig. 31).
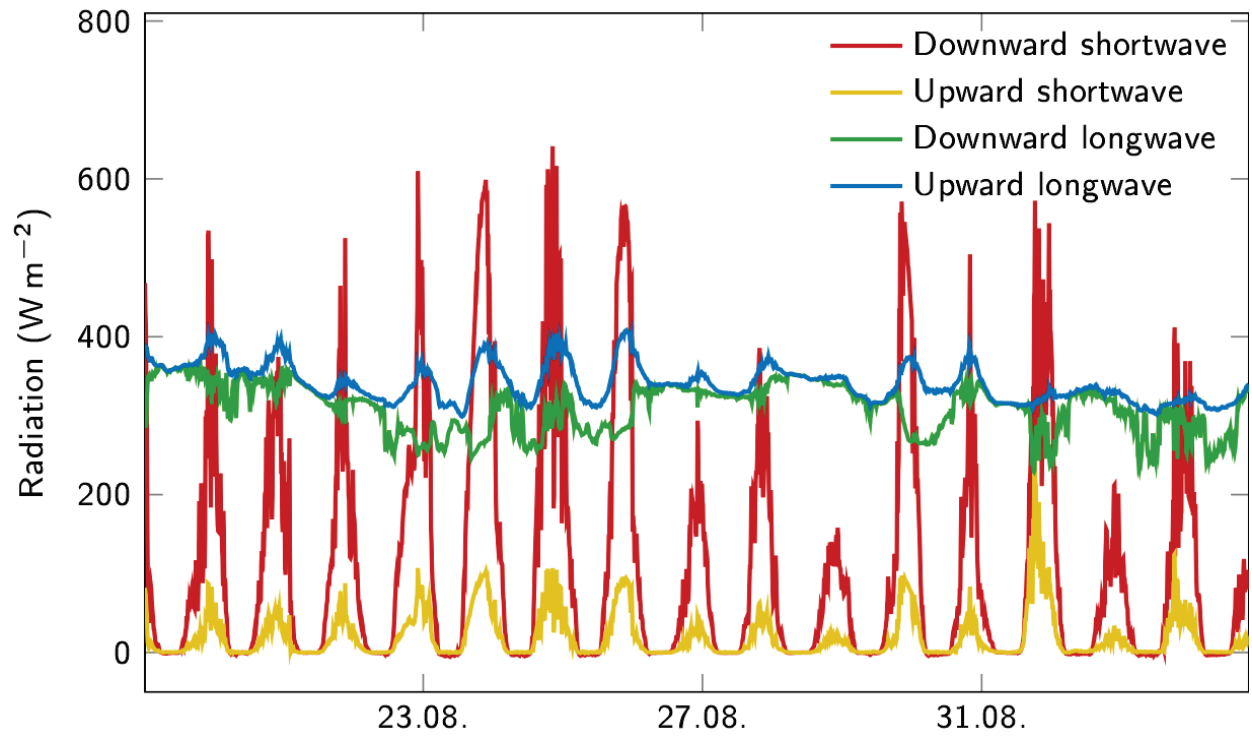
Figure 29: Radiation budget measured at the primary climate station.
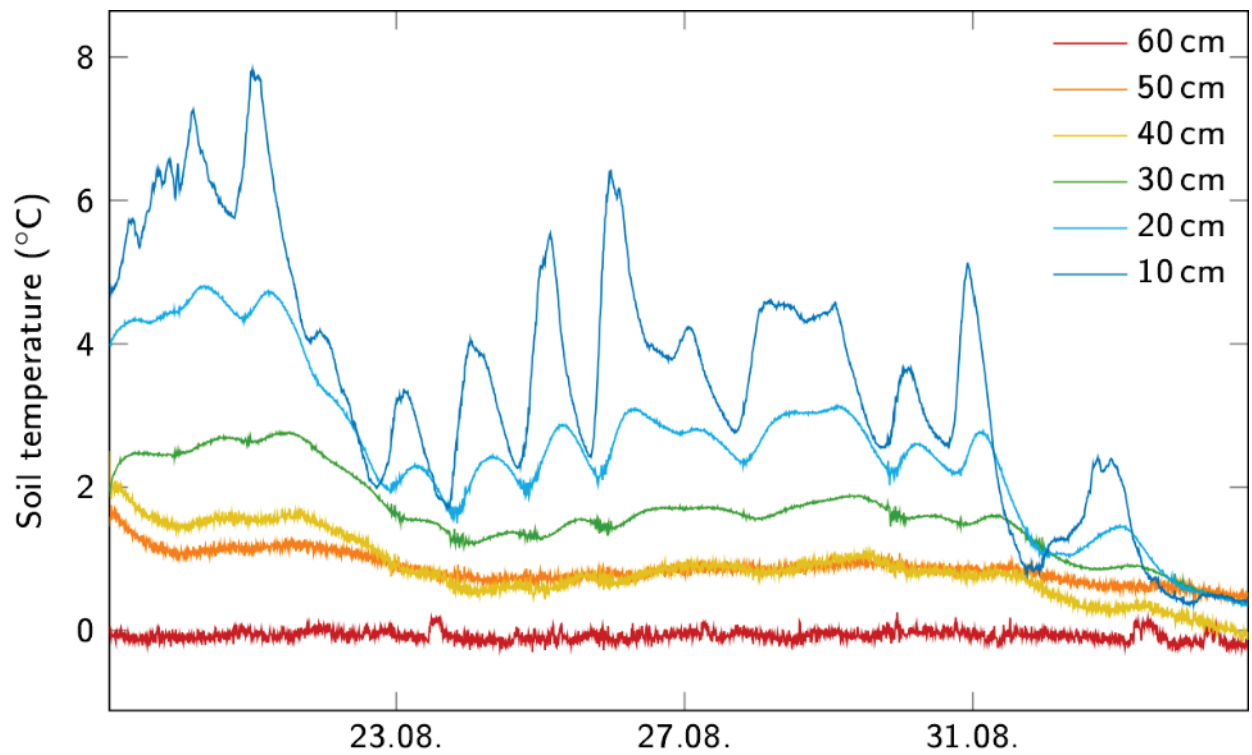
Figure 30: Soil temperatures measured every 10 minutes at 6 different depths at the primary climate station.
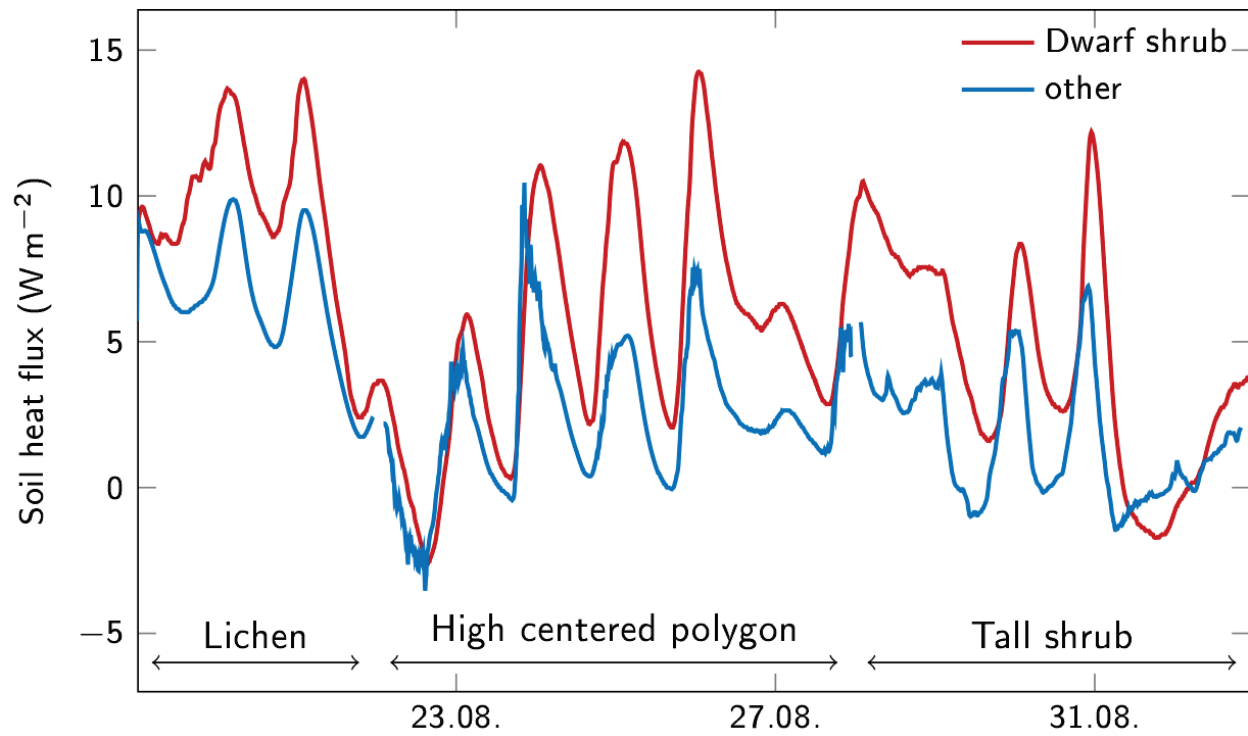
Figure 31: Soil heat flux below different vegetation types measured at the primary climate station above dwarf shrubs and the roving climate station at the three positions (lichen tundra, high centered polygon, tall shrub tundra).

CHAPTER 11 – Interaction between vegetation and soil properties in thaw slumps

Grünberg, I. and Boike, J.

Objectives

A general aim of the MOSES campaign is to compare sites with rapid thaw features to general, slow thawing over larger areas. This project aims at a comparison of vegetation and soil parameters within and next to thaw slumps to gain initial insights in how vegetation is influenced by rapid thaw features and how it in turn modifies local conditions by shading and changing the albedo.

Methodology

We recorded vegetation characteristics, soil properties, active layer thickness, albedo and shading at each measurement location. The full list of variables recorded is:
- Vegetation type (e.g. dwarf shrub)
- Main species
- Additional species
- Maximum vegetation height in 1 m²
- Average vegetation height in 1 m²
- Soil cover (e.g. lichen, moss, litter, water)
- Soil temperature (at 5 cm depth)
- Soil thermal conductivity (at 5 cm depth)
- Soil heat capacity (at 1.5 cm depth)
- Soil volumetric water content (at 6 cm depth)
- Active layer thickness
- Albedo
- Shading

Additionally, we collected active layer and permafrost soil parameters in several soil pits and boreholes (Table 4). The soil and permafrost samples will be analyzed for the following parameters
- Texture/grain size
- Carbon/Nitrogen/Sulphur ratio
- Total organic content
- Ice content
- Microbial composition
- Carbon dating using the MICADAS C-14 facilities at AWI
- Biogenic volatile organic carbon (in collaboration with CENPERM, Copenhagen)

We measured 6-10 points on transects across three thaw slumps and 2-3 points nearby for comparison. In addition, we measured 23 points at 11 different vegetation types to quantify the variability caused by vegetation close to Trail Valley Creek (Table 4, Fig. 32). As soil and climate parameters depend strongly on weather conditions, we will use the data from a climate station (see Section 3.3) as a reference.

Table 4: Measurement locations at, beside, and above the thaw slumps and measurement locations in different vegetation units at Trail Valley Creek.

Station	Date	Latitude (°N)	Longitude (°W)	Notes
Lake 6	20.08.2018	69.03329	133.25422	12 measurement points, 4 soil pits, 2 permafrost cores
Lake 11	24.08.2018	68.75437	133.46662	9 measurement points, 5 soil pits
Lake 12	25.08.2018	68.75805	133.51940	8 measurement points, 4 soil pits
Trail Valley Creek	27.08.2018	68.74848	133.52140	23 measurement points, no soil properties
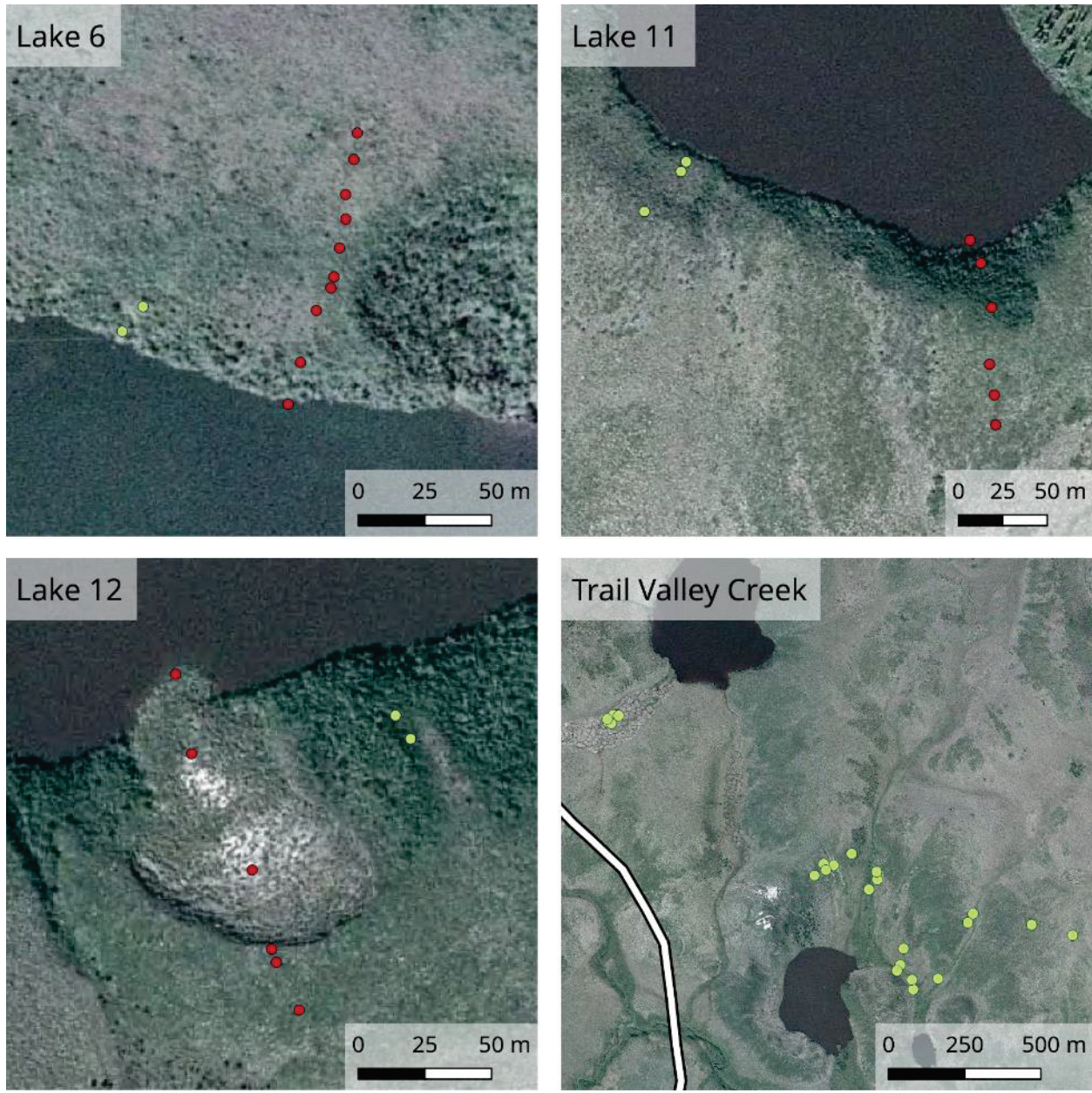
Figure 32: Location of all single measurement points on transects across thaw slumps (red) and at reference locations with different vegetation types (green). Source of background images: Northwest Territories, Centre for Geomatics.

Preliminary Results

We observed significant differences between vegetation and active layer properties within the thaw slumps as compared to above or beside the thaw slump. As an example, we show results of soil temperature, soil moisture and active layer thickness for all points of the three categories (Fig. 33). Thaw slumps have warmer and wetter soil and deeper active layers than the reference locations beside or above the slumps. It should be noted that we could not measure active layer depths of more than 100 cm, which are quite likely within the thaw slumps.
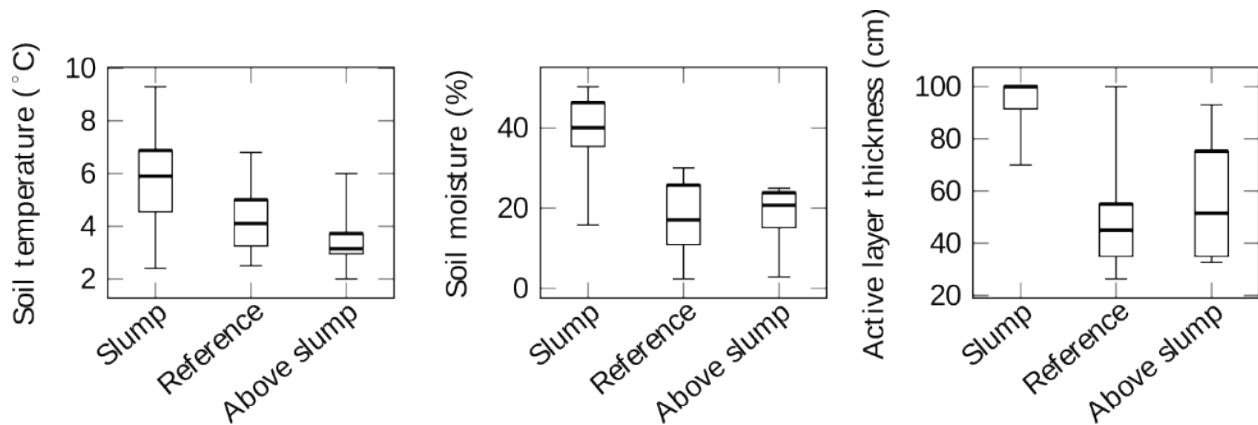
Figure 33: First results of the active layer properties within the thaw slumps, on transect points above and reference points beside the slump.

CHAPTER 12 – Aerial survey and structure from motion

Lange, S. and Boike, J.

Fieldwork Period and Location

From August 13 to September 02, 2018 in Mackenzie River Delta.

Objective

With the drone we recorded images of periglacial landforms (thermokarst lakes, thaw slumps etc.), which have a presumably high erosion potential. By recording the elements from different angles (varying the altitude, camera movement and position relative to the element), 3D models of the observed elements will be generated using the structure from motion (SfM) approach. For georeferencing, Ground Control Points (GCPs) were constructed of weather-resistant material (Fig. 34) and were measured with a differential GPS (dGPS) in RTK-mode.
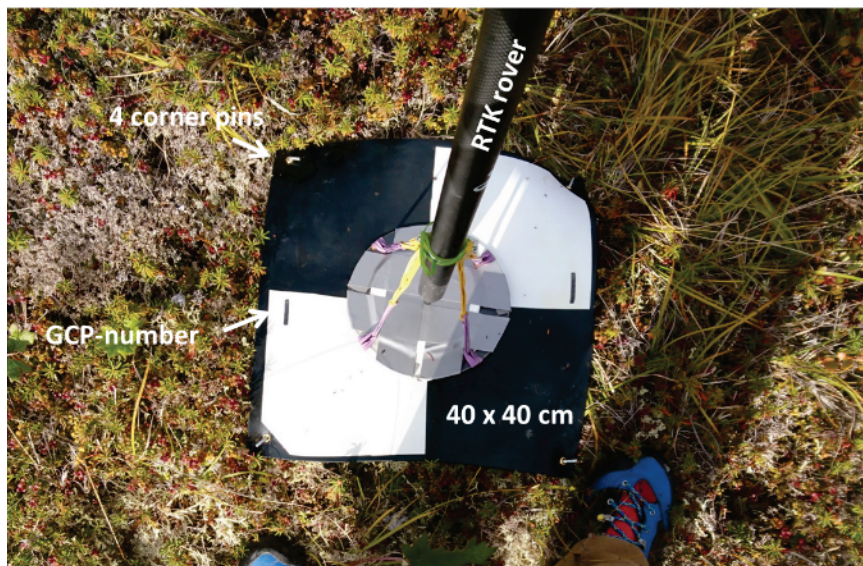
Figure 34: Ground control point (GCP).

Methodology (and/or) Fieldwork Summary

The device for our measurements was a DJI Mavic Pro (Fig. 35). The drone is a very lightweight quadcopter. It is controlled via smartphone and "double grid mission" of Pix4D Capture (Android-4.3.0) (Fig. 36) for flight plans and for the control itself. All flight heights were 30 m above ground (starting point). The overlapping of the RGB-pictures was 70% in each direction. The creation of a point cloud using "structure from motion" is done by the software Agisoft PhotoScan Professional.

Figure 35: Mavic Pro drone.

Figure 36: Flight plan of Pix4D Capture.

Preliminary Results

As a first example, the small thaw slump of Lake 11-II from August 24, 2018 was processed. After the alignment of all jpeg-pictures (389), with a resolution of 3000 x 4000 pixels, a sparse point cloud was calculated. Subsequently, a dense point cloud was calculated (Fig. 37) and the digital elevation model of the thaw slump was generated (Fig. 38).

Figure 37: 3D dense point cloud of one thaw slump at Lake 11-II on Aug 24, 2018.
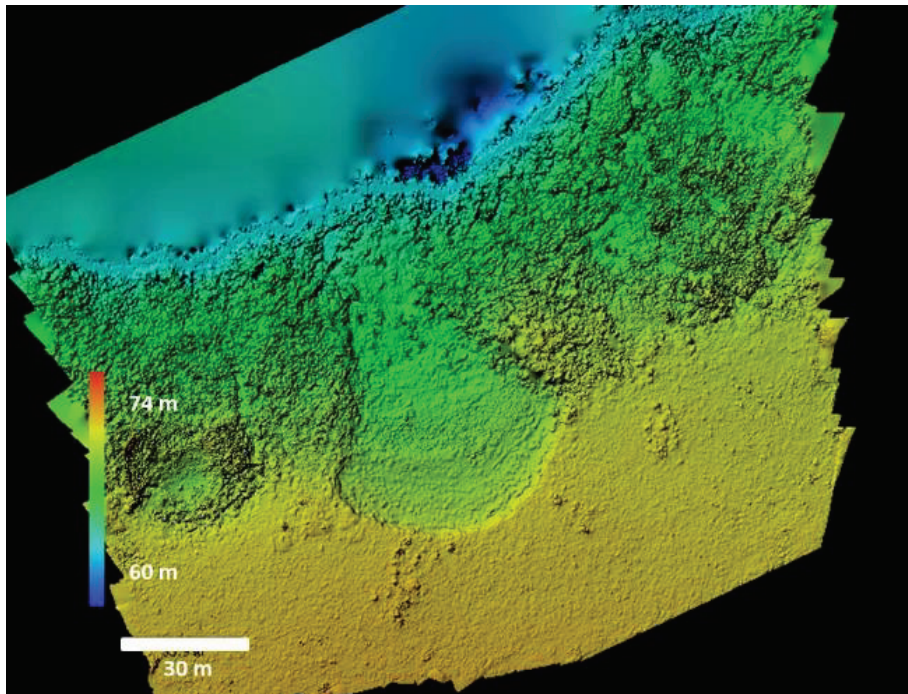
Figure 38: Processed digital elevation model (DEM) of one thaw slump on Lake 11-II on Aug 24, 2018.

Table 5: List of surveys, number of ground control points and pictures.

Survey	Date	Latitude (°N)	Longitude (°W)	GCPs	Number of pictures
Road	18.08.2018	68.75177	133.54572	8	380
Lake 6	20.08.2018	68.75580	133.47650	16	858
Lake 11-I	24.08.2018	68.75415	133.46522	5	821
Lake 11-II	24.08.2018	68.75415	133.46522	5	389
Lake 12	25.08.2018	68.7578	133.52003	5	794

CHAPTER 13 – GNSS measurements - new validation records and repetition

Lange, S. and Boike, J.

Fieldwork Period and Location

From August 13 to September 02, 2018 in Trail Valley Creek Research Station.

Objectives

For validation purposes (e.g. SAR/ALS data) GNSS reference points of the terrain were gathered as well as a description of surface/micro topography and pictures.

Methodology and Fieldwork Summary

Nearly every spot of this expedition was measured with the GNSS, either to repeat previous measurements or the gather new records. Table 6 shows an overview of the amount of all measurements. To keep the rover rod from sinking into the ground and ensure comparable results, the plate shown in Figure 39 (right) was used for the GNSS measurements. For all measurements close to Trail Valley Creek the GNSS base station was setup over a known point, BS1 (560814.0450, 7626306.8380, 79.8708; WGS 84/UTM N8), see Figure 39 (middle). For all other points we used reference points from the construction of the ITH-road, which are spaced regularly along the road (Fig. 39 (left)). The coordinates of these points are available from the government website of Northwest Territories. The Leica antennas GS18 (rover) and GS16 (base station) operate together in real-time kinematic (RTK) mode. The vertical accuracy is 15 mm and horizontally it is 8 mm. After the expedition we used the Precise Point Positioning (PPP) tool from the Canadian Geodetic Survey (CGS) of Natural Resources Canada to correct the base station positions and these corrections were then propagated to the rover positions.
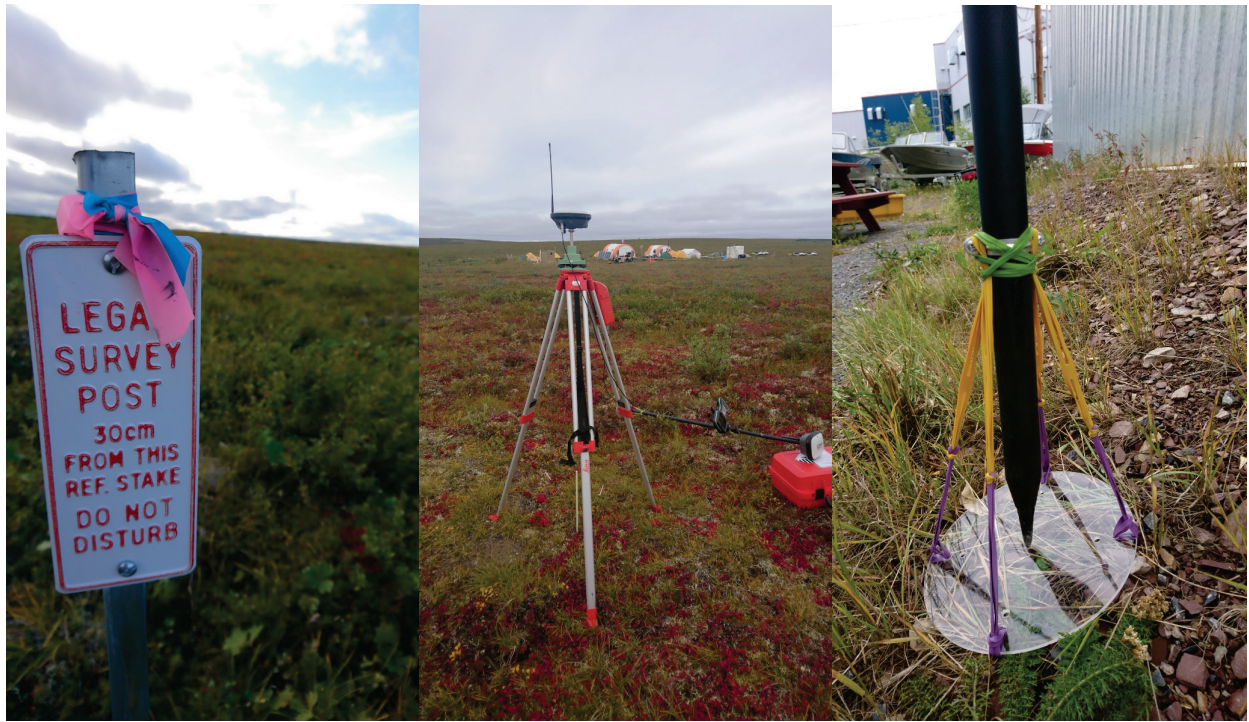
Figure 39: left) "Known" points along the Inuvik-Tuktoyaktuk Highway; middle) Base station for RTK close to Trail Valley Creek; right) plate extension of the rover, to get the surface height on soft surfaces.

Table 6: List of GNSS-measurements.

Sample	Date (from)	Date (to)	Comments	Amount
iButtons	23.08.2018	25.08.2018	See Figure 19	51
Ground Control Points	18.08.2018	25.08.2018	See Table 5	39
Subsidence sticks	22.08.2018	22.08.2018	PermarSAR repeating data	24
Reference transect data	22.08.2018	26.08.2018	6 transects	260
Reference road data	18.08.2018	18.08.2018	2 transects	55
Vegetation transect data	18.08.2018	25.08.2018	See Figure 31	26
Additional points	18.08.2018	26.08.2018	Base station, Corner reflectors, marker, trees, water level	33

CHAPTER 14 – Airborne Laser Scanning (ALS) Point Clouds of Trail Valley Creek and Inuvik-Tuktoyaktuk Highway (ITH)

Boike, J., Hartmann, J., Lange, S., Hartig, B. and Helm, V.

Airborne Laser Scanning in Northwest Territories, Canada, took place in August 2018 over the Trail Valley Creek (TVC) research watershed (August 20, 2018) and the Inuvik-Tuktoyaktuk Highway (August 28, 2018). Point cloud data were acquired with a Riegl LMS-Q680i airborne laser scanner on board the Alfred Wegener Institute's POLAR-5 science aircraft. The location and extent of the dataset are displayed in Figure 2. This flight survey was a repeat survey of the 2016 airborne POLAR-5 mission (Anders et al., 2018) with the aim to detect permafrost degradation (vertical and horizontal). The ALS survey parameters were as follows: 200 kHz pulse repetition rate, a flying altitude of about 2900 ft a.g.l, a flying speed of ~120 kn and a swath width of about 900 m. Attributes that were collected are amplitude, echo width, echo information (echo number and count). The GNSS data were acquired in 20 Hz resolution with a Novatel OEM4 receiver on board the POLAR-5 aircraft. Future processing will combine the GNSS flight trajectory, INS data and ALS data to determine the georeferenced point cloud. The accuracy of the digital terrain model (DTM) will be tested using GNSS measurements of the ground surface acquired during the field campaign between August 21-27, 2018 at Trail Valley Creek and along the Inuvik-Tuktoyaktuk Highway (see Section 3.5).

Data will be archived in the PANGAEA archive similar to Anders et al. (2018).

References

Anders, K., Antonova, S., Boike, J., Gehrmann, M., Hartmann, J., Helm, V., Höfle, B., Marsh, P., Marx, S., and Sachs, T. 2018. Airborne Laser Scanning (ALS) Point Clouds of Trail Valley Creek, NWT, Canada (2016). Alfred Wegener Institute, Helmholtz Center for Polar and Marine Research, Bremerhaven, PANGAEA, doi:10.1594/PANGAEA.894884.

Appendix A. Aquatic field work station data

Table 7: Water sampling at Lake 3 on August 18, 2018. Chemistry included inorganic nutrients, major cations and anions, organic carbon, stable isotopes Alkalinity (TA) and inorganic carbon (DIC) are described in Chapter 5. In addition, a description of methane sampling and on site measurements of oxygen (O_2 in mg/l), pH and conductivity (con in μS/cm) is described also described.

Station	Latitude (°N)	Longitude (°W)	Notes	Water depth (m)	pH/ Con/ O_2	DOC (μM)	DON (μM)	Nitrate (μM)	Nitrite (μM)	Phosphate (μM)	Silicic Acid (μM)
L3-1	68.7761	133.5409	Chemistry, TA, DIC, methane	1	6.90 / 108 / -	1501.75	49.77	<LOD	0.056	0.249	11.404
L3-2	68.7759	133.5413	Chemistry, TA, DIC, methane	1	6.98 / 108 / -	1498.50	45.00	<LOD	0.071	0.228	11.446
L3-CTD1	68.7759	133.5413	CTD								
L3-3	68.7762	133.5402	Chemistry, TA, DIC, methane	1	6.98 / 106 / -	1491.26	41.96	<LOD	0.080	0.223	11.354
L3-4	68.7766	133.5400	Chemistry, TA, DIC, methane	3	6.79 / 117 / -	1524.10	46.74	0.189	0.084	0.236	12.256
L3-5	68.7769	133.5398	Methane		-						

Table 8: Water sampling at Lake 6 on August 20, 2018. Chemistry included inorganic nutrients, major cations and anions, organic carbon, stable isotopes as outlined in 2.2, 2.3. Alkalinity (TA) and inorganic carbon (DIC) are described in 2.2. Description of methane sampling is outlined in 2.4. On site measurements of oxygen (O_2 in mg/l), pH and conductivity (con in µS/cm) is described in 2.2.

Station	Latitude (°W)	Longitude (°W)	Notes	Water depth [m]	pH/ Con/ O_2	DOC (µM)	DON (µM)	Nitrate (µM)	Nitrite (µM)	Phosphate (µM)	Silicic Acid (µM)
L6-1	69.0313	133.2572	Chemistry, TA, DIC, methane	6	7.87 / 134 / 9.51	557.48	30.87	0.187	0.035	0.058	35.702
L6-CTD1	69.0324	133.2547	CTD								
L6-2	69.0314	133.2573	Chemistry, TA, DIC, methane	1	7.98 / 137 / 10.08	568.32	37.41	0.054	0.029	0.053	35.763
L6-3	69.0313	133.2552	Chemistry, TA, DIC, methane	3	7.99 / 137 / 10.29	560.34	32.71	0.029	0.029	0.042	35.866
L6-4	69.0312	133.2546	Chemistry, TA, DIC, methane	4	8.00 / 137 / 8.52	538.44	34.51	0.346	0.026	0.049	35.745
L6-CTD2	69.0313	133.2545	CTD								
L6-5	69.0313	133.2518	Chemistry, TA, DIC, methane	bottom	8.05 / 137 / 8.5	562.76	32.05	0.062	0.023	0.042	35.272
L6-6	69.0327	133.2542	Chemistry, TA, DIC, methane	1	8.00 / 137 / 8.28	536.11	38.00	0.224	0.02	0.042	35.633
L6-CTD3	69.0326	133.2541	CTD								

Station	Latitude (°W)	Longitude (°W)	Notes	Water depth [m]	pH/ Con/ O_2	DOC (μM)	DON (μM)	Nitrate (μM)	Nitrite (μM)	Phosphate (μM)	Silicic Acid (μM)
L6-7	69.0305	133.2537	Chemistry, TA, DIC, methane	1	8.02 / 136 / 9.55	524.10	40.65	0.213	0.025	0.043	35.459
L6-CTD4	69.0307	133.2541	CTD								
L6-8	69.0292	133.2554	Chemistry, TA, DIC, methane	1	8.04 / 137 / 8.27	541.07	44.80	0.218	0.026	0.04	35.118
L6-CTD5	69.0291	133.2553	CTD								

Table 9: Water sampling at Lake 9 on August 28, 2018. Chemistry included inorganic nutrients, major cations and anions, organic carbon, stable isotopes, Alkalinity (TA) and inorganic carbon (DIC) are described in Chapter 5. In addition, a description of methane sampling and on site measurements of oxygen (O_2 in mg/l), pH and conductivity (con in µS/cm) is described also described.

Station	Latitude (°N)	Longitude (°W)	Notes	Water depth (m)	pH/ Con/ O_2	DOC (µM)	DON (µM)	Nitrate (µM)	Nitrite (µM)	Phosphate (µM)	Silicic Acid (µM)
L9-1R	69.0068	133.3634	Chemistry, TA, DIC, methane	4	7.74 / 188 / 9.47	982.79	45.98	<LOD	0.03	0.054	56.607
L9-CTD1	69.0068	133.3633	CTD profile								
L9-2	69.0068	133.3634	Chemistry, TA, DIC, methane	1	7.92 / 186 / 9.6	989.82	30.77	<LOD	0.038	0.055	56.325
L9-3	69.0072	133.3637	Chemistry, TA, DIC, methane, CTD-2	1	7.98 / 186 / 9.6	988.43	60.40	<LOD	0.029	0.05	56.52
L9-CTD2	69.0072	133.3638	CTD profile								
L9-4	69.0076	133.3644	Chemistry, TA, DIC, methane	1	7.97 / 185 / 10.06	993.29	34.99	<LOD	0.03	0.055	56.964
L9-CTD3	69.0076	133.3644	CTD profile								
L9-5	69.0070	133.3663	Chemistry, TA, DIC, methane	4	7.81 / 185 / 10.42	983.74	32.28	<LOD	0.031	0.05	56.926
L9-CTD4	69.0070	133.3661	CTD profile								
L9-6	69.0070	133.3661	Chemistry, TA, DIC, methane	1	8.00 / 185 / 9.67	1100.08	105.31	<LOD	0.03	0.044	56.96
L9-7	69.0073	133.3651	Chemistry, TA, DIC, methane	3	7.99 / 185 / 10.08	980.88	37.61	<LOD	0.027	0.056	57.021
L9-CTD5	69.0074	133.3651	CTD profile								
L9-8	69.0073	133.3651	Chemistry, TA, DIC, methane	1	7.97 / 186 / 10.07	965.81	34.62	<LOD	0.026	0.046	56.975

Station	Latitude (°N)	Longitude (°W)	Notes	Water depth (m)	pH/ Con/ O₂	DOC (μM)	DON (μM)	Nitrate (μM)	Nitrite (μM)	Phosphate (μM)	Silicic Acid (μM)
L9-9	69.0073	133.3630	Chemistry, TA, DIC, methane	1	8.04 / 186 / 9.27	963.14	32.23	<LOD	0.026	0.057	56.551
L9-CTD6	69.0073	133.3631	CTD profile								
L9-10	69.0073	133.3623	Chemistry, TA, DIC, methane	0.5	8.01 / 186 / 9.55	969.82	43.35	<LOD	0.03	0.05	56.577
L9-CTD7	69.0072	133.3624	CTD profile								
L9-AS1	69.0070	133.3634	Air sample								
L9-C1	69.0068	133.3634	Sediment core								
L9-C2	69.0070	133.3636	Sediment core								

Table 10: Water sampling at Tuktoyaktuk Peninsula Point on August 23, 2018. Chemistry included inorganic nutrients, major cations and anions, organic carbon, and stable isotopes Alkalinity (TA) and inorganic carbon (DIC) are described in Chapter 5. In addition, a description of methane sampling and on site measurements of oxygen (O_2 in mg/l), pH and conductivity (con in µS/cm) is described also described.

Station	Latitude (°N)	Longitude (°W)	Notes	Water depth (m)	pH/ Con/ O_2	DOC (µM)	DON (µM)	Nitrate (µM)	Nitrite (µM)	Phosphate (µM)	Silicic Acid (µM)
T1-S1	69.4123	133.1227	Chemistry, TA, DIC, methane	N/A	7.88 / 9 / 8.76	343.10	32.60	3.044	0.033	0.108	42.505
T1-CTD1	69.4123	133.1227	CTD profile								
T1-S2	69.4140	133.1222	Chemistry, TA, DIC, methane	N/A	7.84 / 1811 / 8.14	345.20	42.65	2.847	0.03	0.102	43.205
T1-CTD2	69.4140	133.1222	CTD profile								
T1-S3	69.4161	133.1210	Chemistry, TA, DIC, methane	N/A	7.87 / 6810 / 8.41	381.44	49.77	3.286	0.027	0.107	45.148
T1-CTD3	69.4161	133.1210	CTD profile								
T1-S4	69.4184	133.1197	Chemistry, TA, DIC, methane	N/A	7.87 / 9950 / 9.1	322.31	25.64	3.032	0.031	0.111	41.728
T1-CTD4	69.4184	133.1197	CTD profile								
T1-S5	69.4187	133.1284	Chemistry, TA, DIC, methane	N/A	8.54 / 7780 / -	346.54	37.11	3.152	0.025	0.101	43.996
T1-CTD5	69.4187	133.1284	CTD profile								
T1-S6	69.4163	133.1290	Chemistry, TA, DIC, methane	N/A	7.84 / 11910 / 7.87	323.08	33.99	2.85	0.038	0.12	39.258
T1-CTD6	69.4163	133.1290	CTD profile								
T1-S7	69.4140	133.1289	Chemistry, TA, DIC, methane	N/A	7.86 / 3690 / 8.36	345.96	26.12	2.806	0.038	0.089	43.274
T1-CTD7	69.4140	133.1289	CTD profile								
T1-S8	69.4120	133.12860	Chemistry, TA, DIC, methane	N/A	7.86 / 1541 / 8.91	390.02	36.07	3.117	0.037	0.077	47.749
T1-CTD8	69.4120	133.1286	CTD profile								
T1-S9	69.4118	133.1361	Chemistry, TA, DIC, methane	N/A	7.87 / 20 / 8.47	369.84	31.48	3.049	0.031	0.078	47.142

Station	Latitude (°N)	Longitude (°W)	Notes	Water depth (m)	pH/ Con/ O₂	DOC (µM)	DON (µM)	Nitrate (µM)	Nitrite (µM)	Phosphate (µM)	Silicic Acid (µM)
T1-CTD9	69.4118	133.1361	CTD profile								
T1-S10	69.4160	133.1365	Chemistry, TA, DIC, methane	N/A	7.88 / 8290 / 8.7	787.21	163.93	3.032	0.029	0.099	43.547
T1-CTD10	69.4160	133.1365	CTD profile								
T1-S11	69.4138	133.1366	Chemistry, TA, DIC, methane	N/A	7.78 / 990 / -	314.26	32.37	2.714	0.03	0.115	39.18
T1-CTD11	69.4187	133.1359	CTD profile								
T1-S12	69.4187	133.1359	Chemistry, TA, DIC, methane	N/A	7.63 / 13890 / 7.74	368.09	41.94	2.904	0.033	0.096	44.815
T1-CTD12	69.4187	133.1359	CTD profile								

Table 11: Water sampling at Tuktoyaktuk Island on August 24, 2018. Chemistry included inorganic nutrients, major cations and anions, organic carbon, stable isotopes, Alkalinity (TA) and inorganic carbon (DIC) are described in Chapter 5. In addition, a description of methane sampling and on site measurements of oxygen (O_2 in mg/l), pH and conductivity (con in μS/cm) is described also described.

Station	Latitude (°N)	Longitude (°W)	Notes	Water depth (m)	pH/ Con/ O_2	DOC (μM)	DON (μM)	Nitrate (μM)	Nitrite (μM)	Phosphate (μM)	Silicic Acid (μM)
T2-S1	69.4632	132.9981	Chemistry, TA, DIC, methane	1	7.92 / 17370 / 8.24	304.20	32.06	1.655	0.041	0.121	31.172
T2-S2	69.4633	132.9983	Chemistry, TA, DIC, methane	4	7.93 / 22300 / 7.99	255.94	40.14	3.775	0.041	0.132	29.321
T2-S3	69.4634	132.9982	Chemistry, TA, DIC, methane	7	7.95 / 23100 / 8.13	248.89	20.28	1.232	0.035	0.166	24.496
T2-CTD1	69.4631	132.9981	CTD-profile								
T2-S4	69.4621	133.0070	Chemistry, TA, DIC, methane	1.5	7.95 / 20800 / 7.38	258.61	27.06	1.372	0.032	0.152	27.24
T2-CTD2	69.4620	133.0069	CTD-profile								
T2-S5	69.4604	133.0160	Chemistry, TA, DIC, methane	1.5	7.95 / 20500 / 8.60	267.39	34.07	1.395	0.032	0.148	27.636
T2-CTD3	69.4603	133.0160	CTD-profile								
T2-S6	69.4583	133.0241	Chemistry, TA, DIC, methane	1	7.59 / 18580 / 7.87	271.19	30.56	1.645	0.031	0.132	30.041
T2-CTD4	69.4583	133.0239	CTD-profile								
T2-S7	69.4566	133.0140	Chemistry, TA, DIC, methane	1.5	7.95 / 18720 / 9.19	318.69	25.85	1.743	0.031	0.135	30.101
T2-CTD5	69.4565	133.0140	CTD-profile								
T2-S8	69.4571	133.0041	Chemistry, TA, DIC, methane	1.5	7.93 / 18580 / 8.47	304.00	22.03	1.629	0.036	0.129	30.179
T2-CTD7, 6	69.4569	133.0042	CTD-profile								
T2-S9	69.4585	132.9974	Chemistry, TA, DIC, methane	1.5	- / 19030 / 8.02	334.90	23.10	1.54	0.033	0.132	29.491

Station	Latitude (°N)	Longitude (°W)	Notes	Water depth (m)	pH/ Con/ O₂	DOC (μM)	DON (μM)	Nitrate (μM)	Nitrite (μM)	Phosphate (μM)	Silicic Acid (μM)
T2-S10	69.4610	132.9920	Chemistry, TA, DIC, methane	9	7.93 / 23100 / 7.73	598.86	219.83	1.173	0.035	0.163	24.464
T2-CTD8	69.4607	132.9925	CTD-profile								
T2-S11	69.4606	132.9927	Chemistry, TA, DIC, methane	5	- / - / 7.74	249.27	25.91	1.184	0.032	0.157	24.539
T2-S12	69.4608	132.9923	Chemistry, TA, DIC, methane	1.5	7.91 / 20000 / 7.3	267.77	32.25	1.44	0.031	0.133	28.632

Table 12: Water sampling at Tuktoyaktuk Harbour on August 25, 2018. Chemistry included inorganic nutrients, major cations and anions, organic carbon, stable isotopes, Alkalinity (TA) and inorganic carbon (DIC) are described in Chapter 5. In addition, a description of methane sampling and on site measurements of oxygen (O_2 in mg/l), pH and conductivity (con in µS/cm) is described also described.

Station	Latitude (°N)	Longitude (°W)	Notes	Water depth (m)	pH/ Con/ O_2	DOC (µM)	DON (µM)	Nitrate (µM)	Nitrite (µM)	Phosphate (µM)	Silicic Acid (µM)
T3-S1	69.4195	132.9727	Chemistry, TA, DIC, methane	20	7.41 / 37800 / 3.75	353.02	137.66	17.494	0.041	0.224	35.925
T3-S2	69.4195	132.9727	Chemistry, TA, DIC, methane	10	7.38 / 39400 / 3.17	190.29	41.74	21.388	0.04	0.673	39.204
T3-S3	69.4195	132.9727	Chemistry, TA, DIC, methane	5	7.98 / 14580 / 8.11	451.92	36.79	2.021	0.027	0.097	34.297
T3-S4	69.4196	132.9727	Chemistry, TA, DIC, methane	1	8.10 / 6870 / 9.57	272.51	18.17	1.021	0.026	0.064	40.982
T3-CTD1	69.4195	132.9727	CTD-profile	22							
T3-S5	69.4360	132.9732	Chemistry, TA, DIC, methane	20	7.35 / 39800 / 2.19	257.19	47.85	24.178	0.04	0.244	37.771
T3-S6	69.4360	132.9734	Chemistry, TA, DIC, methane	10	7.66 / 29500 / 5.29	149.79	20.52	10.431	0.035	0.196	31.731
T3-S7	69.4360	132.9728	Chemistry, TA, DIC, methane	5	7.72 / 23100 / 6.41	407.86	51.77	8.222	0.033	0.133	35.518
T3-S8	69.4359	132.9732	Chemistry, TA, DIC, methane	1	8.02 / 12300 / 8.11	273.64	27.65	1.877	0.029	0.058	36.491
T3-CTD2	69.4360	132.9730	CTD-profile	21							

Table 13: Water sampling at Mackenzie Estuary on August 27, 2018. Chemistry included inorganic nutrients, major cations and anions, organic carbon, stable isotopes Alkalinity (TA) and inorganic carbon (DIC) are described in Chapter 5. In addition a description of methane sampling and on site measurements of oxygen (O_2 in mg/l), pH and conductivity (con in µS/cm) is described also described.,

Station	Latitude (°N)	Longitude (°W)	Notes	Water depth (m)	pH/ Con/ O_2	DOC (µM)	DON (µM)	Nitrate (µM)	Nitrite (µM)	Phosphate (µM)	Silicic Acid (µM)
T4-S1	69.4035	133.6892	Chemistry, TA, DIC, methane	3	8.13 / 340 / 9.66	418.06	43.54	3.836	0.026	0.093	53.898
T4-S2	69.4047	133.6917	Chemistry, TA, DIC, methane	1	8.19 / 345 / 9.46	419.01	27.40	3.924	0.024	0.088	54.214
T4-CTD1	69.4026	133.6876	CTD-profile								
T4-S3	69.4104	133.7201	Chemistry, TA, DIC, methane	2	8.17 / 345 / 11.6	403.37	31.19	3.928	0.024	0.072	54.542
T4-CTD2	69.4089	133.7156	CTD-profile								
T4-S4	69.4193	133.8070	Chemistry, TA, DIC, methane	2	8.17 / 345 / 9.67	390.02	19.48	4.04	0.022	0.075	55.103
T4-CTD3	69.4180	133.8039	CTD-profile								
T4-S5	69.4387	133.8126	Chemistry, TA, DIC, methane	1	8.16 / 346 / 10.23	414.81	27.55	4.007	0.024	0.073	54.473
T4-CTD4	69.4367	133.8089	CTD-profile								
T4-S6	69.4488	133.7151	Chemistry, TA, DIC, methane	1	8.16 / 346 / 9.85	400.32	21.81	4.085	0.023	0.084	54.509
T4-CTD5	69.4475	133.7149	CTD-profile								
T4-S7	69.4540	133.6304	Chemistry, TA, DIC, methane	1	8.18 / 347 / 9.68	395.93	26.69	4.154	0.027	0.075	54.022
T4-CTD6	69.4528	133.6261	CTD-profile								
T4-S8	69.4198	133.6696	Chemistry, TA, DIC, methane	N/A	8.15 / 345 / 9.45	395.17	22.48	4.083	0.018	0.071	54.241

Station	Latitude (°N)	Longitude (°W)	Notes	Water depth (m)	pH/ Con/ O$_2$	DOC (μM)	DON (μM)	Nitrate (μM)	Nitrite (μM)	Phosphate (μM)	Silicic Acid (μM)
T4-S9	69.4201	133.6709	Chemistry, TA, DIC, methane	N/A	8.16 / 361 / 9.91	391.36	20.73	4.07	0.027	0.059	54.614
T4-CTD7	69.4194	133.6645	CTD-profile								
T4-S10	69.3845	133.6787	Chemistry, TA, DIC, methane	4	8.16 / 362 / 10.02	407.76	26.79	4.035	0.024	0.071	54.395
T4-S11	69.3850	133.6795	Chemistry, TA, DIC, methane	1	N/A	415.01	24.36	4.066	0.029	0.074	54.771
T4-CTD8	69.3829	133.6760	CTD-profile								
T4-S12	69.4012	133.5539	Chemistry, TA, DIC, methane, no DOC	N/A	N/A						
T4-CTD9	69.3998	133.5552	CTD-profile								

Table 14: Water sampling at Mackenzie River on September 3, 2018. Chemistry included inorganic nutrients, major cations and anions, organic carbon, stable isotopes, Alkalinity (TA) and inorganic carbon (DIC) are described in Chapter 5. In addition a description of methane sampling and on site measurements of oxygen (O_2 in mg/l), pH and conductivity (con in µS/cm) is described also described.

Station	Latitude (°N)	Longitude (°W)	Notes	Water depth (m)	pH/ Con/ O_2	DOC (µM)	DON (µM)	Nitrate (µM)	Nitrite (µM)	Phosphate (µM)	Silicic Acid (µM)
R-1	69.2430	135.2040	Chemistry, TA, DIC, methane, no cDOM	20	8.12 / 344 / 9.15	452.20	26.64	4.888	0.026	0.086	55.699
R-2	69.2430	135.2040	Chemistry, TA, DIC, methane	1	8.13 / 344 / 9.74	421.03	25.07	4.954	0.024	0.076	55.83
R-CTD1	69.2430	135.2040	CTD-profile								
R-3	69.2017	135.0893	Chemistry, TA, DIC, methane, no cDOM	6	8.13 / 193 / 8.02	440.25	48.48	4.922	0.024	0.068	55.701
R-4	69.2019	135.0883	Chemistry, TA, DIC, methane, no cDOM	1	8.14 / 340 / 9.14	438.46	22.17	4.923	0.034	0.07	55.719
R-CTD2	69.2018	135.0915	CTD-profile								
R-5	69.1786	135.1546	Chemistry, TA, DIC, methane, no cDOM	20	8.12 / 336 / 8.42	435.38	37.14	4.925	0.023	0.073	55.868
R-6	69.1786	135.1546	Chemistry, TA, DIC, methane, no cDOM	3	8.11 / 344 / 9.74	460.16	29.98	4.943	0.031	0.073	55.784
R-CTD3	69.1787	135.1527	CTD-profile								

Station	Latitude (°N)	Longitude (°W)	Notes	Water depth (m)	pH/ Con/ O$_2$	DOC (µM)	DON (µM)	Nitrate (µM)	Nitrite (µM)	Phosphate (µM)	Silicic Acid (µM)
R-7	69.1086	134.8969	Chemistry, TA, DIC, methane, no cDOM	1	8.17 / 337 / 10.44	418.71	27.91	3.742	0.029	0.059	54.034
R-CTD4	69.1091	134.9009	CTD-profile								
R-8	69.1063	134.8293	Chemistry, TA, DIC, methane, no cDOM	1	8.16 / 341 / 9.79	476.23	23.79	4.313	0.03	0.048	53.979
R-9	68.6892	134.1399	Chemistry, TA, DIC, methane, no DOC, no cDOM	1	8.15 / 337 / 9.95	465.95	24.11	4.258	0.032	0.046	53.884
R10	68.6333	134.0763	Chemistry, TA, DIC, methane, no DOC	1	8.15 / 336 / 10.15	463.87	41.09	4.045	0.034	0.036	53.39
R-CTD5	68.6334	134.0761	CTD-profile								
RS-1	69.2011	135.0904	Sediment methane & porosity								
RS-2	69.1082	134.8989	Sediment methane & porosity								
RS-3	N 68.6336	W 134.0765	Sediment methane & porosity								

Appendix B. Online data portal

Most data collected during this field program are available online at https://dashboard.awi.de/?dashboard=8064. Available datasets include radiation over permafrost landscape, and methane and CO_2 concentrations over thermokarst lakes.
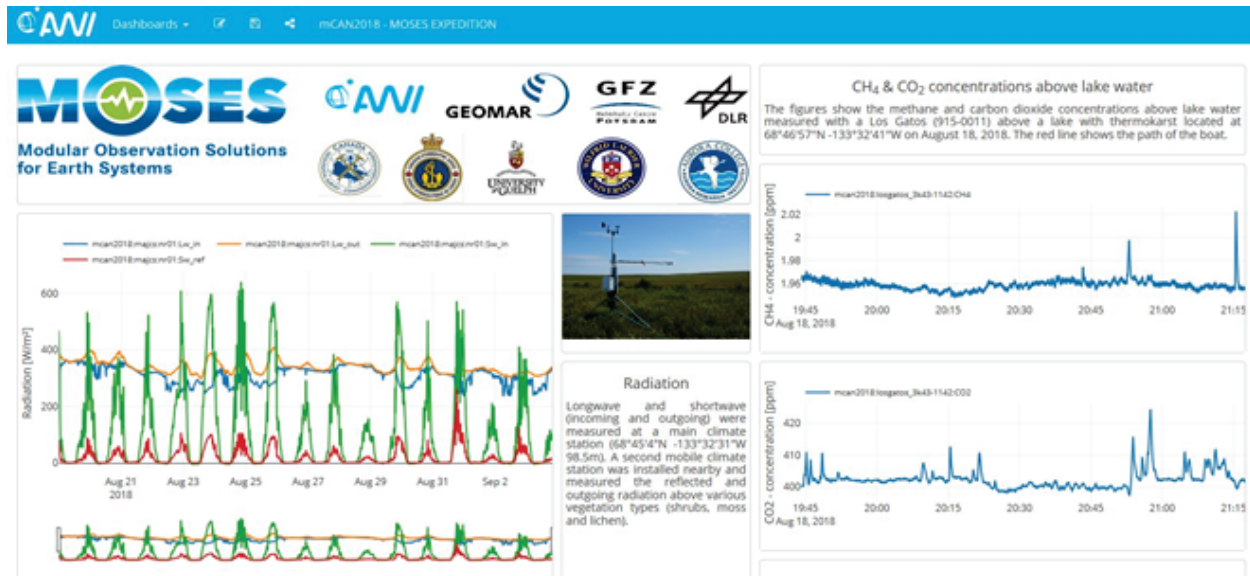

Figure 40: Example of data of radiation sensors over permafrost landscape and of methane and CO_2 concentrations above thermokarst lakes.

Table 15: Steps to download data and parameters online using the dashboard: https://dashboard.awi.de/data-xxl/overview.jsp; Steps: use filter input to choose dataset → scroll down to "request data" → choose begin and end of campaign (2018-08-18 - 2018-09-03) → build request.

Institute	Sensor/ platform	Parameters	Sensor.awi	Filter
AWI	ctd	water temperature	https://sensor.awi.de/?urn=laboratory:mcan2018:ctd_25564	mcan2018:ctd_25564
		water depth		
		water conductivity		
		water density		
		water salinity		
Geomar	ctd	water depth	https://sensor.awi.de/?urn=laboratory:mcan2018:ctd_ysi_exo1_17j100702	mcan2018:ctd_ysi
		water conductivity		
		water salinity		
		water temperature		
		dissolved oxygen		
Geomar	prooceanos	methane	https://sensor.awi.de/?urn=laboratory:mcan2018:geomar_prooceanus_mini_methane_sensor_3747725	mcan2018:geomar_prooceanus
		detector temperature		
		current A/D		
		reference A/D		
AWI	losgatos	ambient temperature	https://sensor.awi.de/?urn=laboratory:mcan2018:losgatos_3k43-1142	mcan2018:losgatos_3k43-1142
		methane concentrations		
		CO_2 concentrations		
		depth		
		gas pressure		
		H_2O concentration		
AWI	climate station (major)	soil heat flux	https://sensor.awi.de/?urn=laboratory:mcan2018:majcs	mcan2018:majcs
		soil temperatures		
		surface temperature		
		air temperature		
		humidity		
		radiation		
		wind		
AWI	climate station (roving)	soil heat flux	https://sensor.awi.de/?urn=laboratory:mcan2018:rovcs	mcan2018:rovcs
		surface temperature		
		humidity		
		radiation		
		wind		

a. Participating and cooperating institutions

Institute	Address
AWI	Alfred-Wegener-Institut, Helmholtz-Zentrum für Polar- und Meeresforschung Postfach 120161 27515 Bremerhaven Germany
GEOMAR	GEOMAR Helmholtz-Zentrum für Ozeanforschung Kiel Wischhofstr. 1-3 24148 Kiel Germany
GFZ	Helmholtz Centre Potsdam GFZ German Research Centre for Geosciences Telegrafenberg 14473 Potsdam Germany
Canadian Partners	
GSC	[a]Geological Survey of Canada-Pacific, Natural Resources Canada, 9860 West Saanich Rd., Sidney, BC, V8L 4B2, Canada [b]Geological Survey of Canada-North, Natural Resources Canada, 601 Booth St., Ottawa, ON, KIA OE8, Canada
RRU	Royal Roads University 2005 Sooke Rd., Victoria, BC V9B 5Y2 Canada
CHS	Canadian Hydrographic Service, Fisheries and Oceans Canada, 867 Lakeshore Rd., Burlington, ON, L7S 1A1, CANADA
ARI	Aurora Research Institute, Aurora Research Institute, 191 Mackenzie Road, PO Box 1450, Inuvik, NT, X0E 0T0, Canada
U Guelph	University of Guelph 50 Stone Road East, Guelph, Ontario, N1G 2W1, Canada

| WLU | Wilfrid Laurier University 75 University Avenue West, Waterloo, Ontario, N2L 3C5, Canada |

b. Expedition participants

Last name	First name	Institute	Profession
Boike	Julia	AWI	Permafrost scientist
Bussmann	Ingeborg	AWI	Biologist
Cable	William	AWI	Technician
Juszak (Grünberg)	Inge	AWI	Hydrologist
Kampmeier	Mareike	GEOMAR	PhD student, Geology
Lange	Stephan	AWI	Data scientist
Nehir	Münevver	GEOMAR	PhD student, Chemistry
Weiss	Tim	GEOMAR	Technician
Couture	Nicole	GSC	Research Scientist
Dallimore	Scott	GSC	Research Scientist
Molloy	Byron	Royal Roads University	Scientist
Dallimore	Audrey	Royal Roads University	Associate Professor